

9-3-2013

Evaluation of hydraulic roughness routines and properties in the presence of vegetation

Abdou Harissou Ouro Bang'na Nassam

Follow this and additional works at: https://digitalrepository.unm.edu/ce_etds

Recommended Citation

Ouro Bang'na Nassam, Abdou Harissou. "Evaluation of hydraulic roughness routines and properties in the presence of vegetation." (2013). https://digitalrepository.unm.edu/ce_etds/77

This Thesis is brought to you for free and open access by the Engineering ETDs at UNM Digital Repository. It has been accepted for inclusion in Civil Engineering ETDs by an authorized administrator of UNM Digital Repository. For more information, please contact disc@unm.edu.

Abdou Harissou Ouro Bang'na Nassam

Candidate

Civil Engineering

Department

This thesis is approved, and it is acceptable in quality and form for publication:

Approved by the Thesis Committee:

Dr. Mark C. Stone, Chairperson

Dr. Andrew Schuler

Dr. Guohui Zhang

Evaluation of Hydraulic Roughness Routines and Properties in the Presence of Vegetation

BY

ABDOU HARISSOU OURO BANG'NA NASSAM

Bachelor of Science
Civil Engineering
University of Minnesota, Twin-Cities, 2010

THESIS

Submitted in Partial Fulfillment of the
Requirements for the Degree of

Master of Science
Civil Engineering

The University of New Mexico
Albuquerque, New Mexico

July 2013

ACKNOWLEDGEMENTS

My Committee:

Dr. Mark Stone, Dr. Andrew Schuler, Dr. Guohui Zhang

Research Scientists and Assistants:

Jeffrey Samson, Tyler Gillihan and Kareem St. Lot

Funding and Technical Support:

NSF-BD-8, HRD#1026412, NM-AMP, Civil-Eng. Hydraulic Laboratory

Unwavering Support from Family:

Ouro Bang'na Nassam and Toovi-Balumuka

TABLE OF CONTENTS

| | |
|---|----|
| Abstract | 1 |
| Introduction..... | 3 |
| Background..... | 5 |
| Methods | 12 |
| Roughness calculator spreadsheet | 12 |
| Uncertainty assessment | 13 |
| Laboratory investigation..... | 15 |
| Results..... | 18 |
| Discussion..... | 28 |
| Conclusion | 31 |
| Future Research | 32 |
| Literature Cited | 34 |
| Appendix A-Nomenclature..... | 36 |
| Appendix B - MatLab Code..... | 37 |
| Appendix C- Roughness Calculation Spreadsheet | 47 |
| Appendix D - Conceptual model development..... | 53 |
| Appendix E - Theoretical basis..... | 61 |

LIST OF FIGURES

| | |
|--|----|
| Figure 1. Friction factor as function of Reynolds number & relative roughness (Munson et al. 2012) | 7 |
| Figure 3. Drag coefficients for a smooth cylinder and sphere as a function of particle Re (Munson et al. 2012) | 8 |
| Figure 2. Boundary layer characteristics on a circular cylinder (Munson et al. 2012)..... | 8 |
| Figure 4. Plant drag force as a function of approach velocity (Freeman et al. 2000)..... | 9 |
| Figure 5. Google aerial image of the SLR USACE project area. | 14 |
| Figure 6. Photograph of SLR channel vegetation at Bennete Bridge (photo by M. Stone)..... | 14 |
| Figure 7. Schematic of a profile view of the experimental flume | 16 |
| Figure 8. ADV in the flume | 16 |
| Figure 9. Variation in Manning's n as a function of LAI and C_{dr} based on Jarvela (2004)..... | 20 |
| Figure 10. Variation in Manning's n as a function of vegetation density and C_d based on Baptist et al. (2007) | 21 |
| Figure 11. Histogram for the Jarvela approach..... | 22 |
| Figure 12. Histogram for the Baptist '07 approach. | 23 |
| Figure 13. Jarvela '04 approach, Manning's n as function of LAI | 24 |
| Figure 14. Jarvela '04 approach, normal depth as function of LAI | 24 |
| Figure 15. Baptist '07 approach, Manning's n as function of $m \cdot D$ | 25 |
| Figure 16. Baptist '07 approach, normal depth as function of $m \cdot D$ | 25 |
| Figure 17. Turbulent kinetic energy (TKE) as a function of location and approach velocity | 26 |
| Figure 18. Integral length scale (L) as a function of location and approach velocity..... | 28 |
| Figure 19. Integral time scale (T) as a function of location and approach velocity | 28 |
| Figure 20: Schematic of the conceptual model..... | 53 |

LIST OF TABLES

| | |
|---|----|
| Table 1. Summary of common methods for estimating vegetation roughness..... | 11 |
|---|----|

Evaluation of Hydraulic Roughness Routines and Properties in the Presence of Vegetation

BY

ABDOU HARISSOU “HARRIS” OURO BANG’NA NASSAM

B.S. CIVIL ENGINEERING, UNIVERSITY OF MINNESOTA, TWIN CITIES 2010

M.S. CIVIL ENGINEERING, UNIVERSITY OF NEW MEXICO 2013

Abstract

Hydraulic roughness in the presence of vegetation is notoriously difficult to predict. However, reliable methods for predicting flow resistance in vegetated channels and floodplains are needed in order to address the needs of modern river engineering. To this end, the objectives of this research were: (1) to evaluate methods for determining hydraulic roughness within open channels in the presence of vegetation, and (2) to advance understanding of the influence of vegetation on the turbulence characteristics of the flow field. Three major activities were completed in order to address these objectives. First, a roughness calculator spreadsheet was developed based on a thorough review of available techniques for predicting hydraulic roughness in the presence of vegetation. The calculator includes the five most cited methods. Second, the roughness calculator and a Monte Carlo based MATLAB codes were used to investigate sensitivity and uncertainty within the techniques. Two of the techniques for predicting roughness were applied to a test case of the San Luis River in Oceanside, California. Third, a flume experiment was conducted to investigate turbulence characteristics in the presence of artificial vegetation elements.

Study results revealed that of the various methods available for estimating hydraulic roughness in the presence of vegetation, two approaches showed the most

promise with respect to data availability and ease of application: – Jarvela (2004) and Baptist et al. (2007). All of the hydraulic roughness estimating techniques showed a high degree of sensitivity to input parameters including descriptions of vegetation density and drag coefficients. Uncertainty in input parameters translated to uncertainties in predictions of hydraulic roughness and flow depth. Thus, future research should aim to improve species-specific estimates of common parameters and techniques for measuring field parameters. Turbulence metrics can provide much insight into the mechanisms in which energy is extracted from the bulk flow as a result of drag forces. This area of research shows promise with respect to developing general models for predicting hydraulic roughness.

Introduction

In spite of countless efforts to curtail the devastating effects of floods, flash flooding remains the leading cause of weather-related deaths in the U.S. according to the Center for Disease Control and Prevention (CDC 2010). Further, according to the National Weather Service Hydrologic Information Center (NWS HIS 2009), the average damage in the U.S. attributed to major floods between 1990 and 2007 was just under \$9 billion per year. Internationally, freshwater floods (excluding coastal events) killed at least 100,000 people and affected over 1.4 billion people over the course of the 20th century (Jonkman 2005).

Humans have long attempted to exert control over rivers to satisfy the immediate needs of society (Nixon 1980), (Phillips 1989), (Kadlec 1990 & Shi *et al.* 1995), (Nepf 1997), Guardo and Tomasello (1995), Kadlec (1990) and Jadhav and Buchberger (1995). However, it is believed that in many cases river engineering has resulted in increased vulnerability to natural disasters by degrading the systems' natural buffering capacity and increasing human exposure to risks (e.g. floodplain development) (e.g. Mustafa 2007, Farber and Costanza *et al.* 1987, Haeuber and Michener 1998). Hence, today's focus has largely shifted away from traditional efforts to control rivers and towards efforts to manage rivers in a more sustainable and integrated fashion.

The challenge, however, lies in the fact that most engineering models and tools were developed to describe heavily engineered systems. The underlying assumptions that work well in engineered settings are often not applicable to natural systems. For example, existing hydrodynamic models assume a constant hydraulic roughness, independent of flow conditions. This gross simplification is not appropriate in natural channels and floodplains where form drag induced by vegetation dominates flow resistance.

The influence of vegetation on stream flow can be considered at both the reach scale and at the watershed scale. At the reach scale, the influence of channel vegetation is increased hydraulic roughness and thus water stage for a given stream discharge. At the watershed scale however, vegetation can act to reduce and slow runoff, attenuate flood-wave movement, and thus reduce flood risks. Riparian zones as well as wetlands also provide many other functions including the provisioning of both aquatic and terrestrial habitats, nutrient exchange and processing (Nixon 1980), and stabilization of sediments (Phillips 1989). Thus, unlike historical thinking where channel vegetation was considered as a nuisance, current projects aim to preserve or enhance vegetation conditions and the ecosystem services associated with functioning riparian zones.

In spite of the important roles of vegetation and the increased desire to maintain or restore channel and floodplain vegetation, the description of fluid dynamics processes and the estimation of hydraulic conditions in the presence of vegetation is complex and still highly uncertain. Vegetation influences the main flow by imparting a drag force from plant elements, which reduces the mean flow within the vegetated regions relative to non-vegetated areas (Kadlec 1990 and Shi *et al.* 1995). In addition to affecting the mean velocity, vegetation also impacts turbulence characteristics and as a result influences the diffusion of mass and momentum. For example, an increase of the turbulence intensity due to the conversion of mean kinetic energy to turbulent kinetic energy within the stem wake is observed, and the predominant turbulent length scale is shifted downward relative to non-vegetated open-channels (Nepf 1997).

Over the past several decades, a number of studies have been carried out to model hydraulic roughness resulting from channel vegetation. For example, Guardo and Tomasello (1995), Kadlec (1990), and Jadhav and Buchberger (1995) have demonstrated

that the Manning's roughness coefficient (n) can be adjusted to evaluate bulk flow conditions. However, these approaches are difficult to apply for a practicing engineer and the require parameters that are difficult to determine for field conditions. Further, the degrees of uncertainty from the various approaches have not been directly investigated.

The objectives of this research were: (1) to evaluate methods for determining hydraulic roughness within open channels in the presence of vegetation, and (2) to advance understanding of the influence of vegetation on the turbulence characteristics of the flow field. The research included a review and evaluation of the various techniques that have been proposed for estimating hydraulic roughness. A spreadsheet-based calculator was developed to facilitate the estimation of hydraulic roughness resulting from vegetation using a number of methods. Further, a Monte Carlo based uncertainty assessment was performed on two of the approaches using a case study for the San Luis Rey in Oceanside, California using MATLAB. Finally, flume experiments with artificial vegetation elements were conducted to improve understanding of vegetation-induced effects on turbulence characteristics. The results of this study will advance understanding of vegetation based hydraulic roughness and also will inform associated numerical modeling studies underway by the research team.

Background

Characterizing hydraulic roughness in open channels and closed conduits has been a research topic dating back more than 100 years. Schlichting (1936) was one the first investigators to study the effect of roughness elements on drag forces and shear stresses from a theoretical perspective. In his classic work, Schlichting proposed that flow resistance can be decomposed into two major components: (1) skin friction and (2)

form drag (pressure gradients). The drag force equation can be decomposed and the coefficients of drag are adjusted based upon the stream geometry and the flow conditions within it. The equation quantifying the total drag force is:

$$F_D = F_f + F_p$$

$$F_D = \frac{1}{2} \rho AV^2 C_{Df} + \frac{1}{2} \rho AV^2 C_{Dp}$$

$$F_D = \frac{1}{2} \rho AV^2 C_D$$

where F_D is the total drag force in the system, F_f is the drag force due to friction, F_p is the drag force due to pressure gradients, A is the characteristic or projected area of the object, V is the flow velocity, ρ is the density of water, C_{Df} represents the drag coefficient due to friction, C_{Dp} represents the drag coefficient due to pressure, and C_D represents the composite drag coefficient.

Within open channels, the most common relationship for relating channel geometry, flow conditions, and hydraulic roughness is the Manning's Equation:

$$V = \frac{K}{n} R^{2/3} S_f^{1/2}$$

where V is the mean flow velocity, n is the Manning's resistance coefficient, K is a unit correction factor of 1.0 For SI units and 1.49 for non-SI units, R is the hydraulic radius, and S_f is the energy grade slope.

Manning's n can be approximated through a range of approaches, but it is almost always considered to be constant for a given channel location – independent of flow condition. The assumption of a constant n value works well in engineered settings because the dominant source of roughness is skin friction (F_f) and thus the form drag (F_p) can be neglected. We know from the classic Moody experiments (Figure 1) that the friction

factor becomes independent of the flow conditions for high Reynolds numbers, as we would expect in an open channel. However, in the presence of vegetation, this conceptual model is no longer applicable. Form drag induced by vegetation elements can become the dominant sources of resistance, and form drag is known to vary significantly with flow condition.

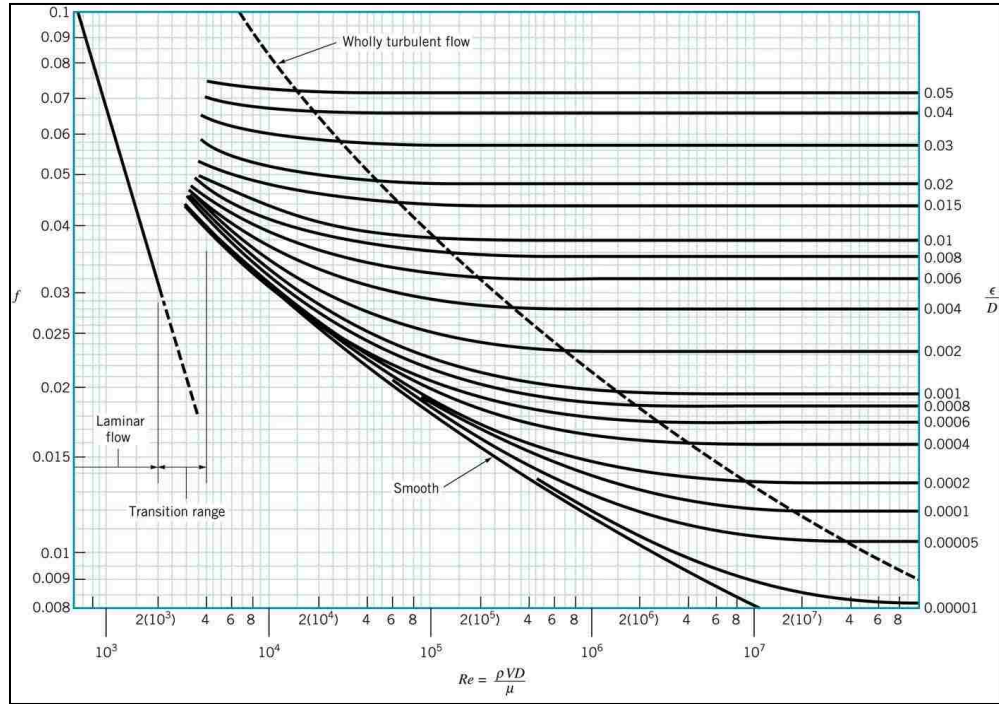
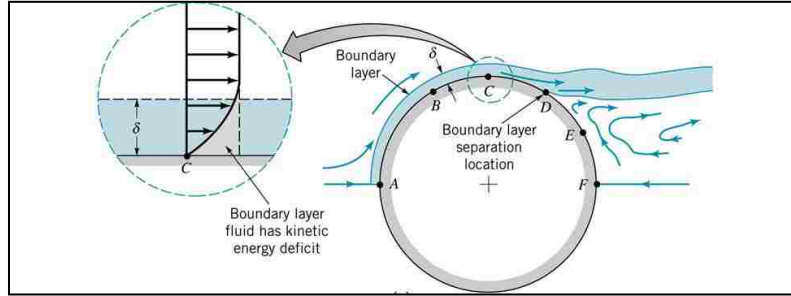


Figure 1. Friction factor as function of Reynolds number & relative roughness (Munson et al. 2012)

As the flow progresses around vegetation stems, it behaves similarly to flow around a cylinder as described in classic fluid mechanics. As shown in Figure 2, boundary layer separation will occur as the fluid passes around the cylinder (or stem) resulting in an imbalance in pressure forces around the element's perimeter. Specifically, a much higher pressure will be realized on the front of the cylinder than on the back of the cylinder. When the pressure is integrated over the element's perimeter, a net force is produced by the flow on the element in the direction of flow. Likewise, an equal resistive force is produced by the element on the flow.



The magnitude of the drag and corresponding resistive forces are strongly influenced by the boundary characteristics, which have been shown to be a function of the Reynolds number (Re). As the Re is increased, the flow contains additional kinetic energy and the boundary layer separation point will occur further along the circumference of the cylinder. Thus, as the Re is increased the drag coefficient is gradually reduced (Figure 3). It is important to note that the Re in this situation is for the roughness element, and thus the characteristic length is the element's diameter, not the flow depth. Thus, the Re is much lower and is typically found to be in the highly variable stage. It is also important to note that although C_D decreases as Re is increased, the overall drag force will still climb with velocity because it is a function of velocity squared.

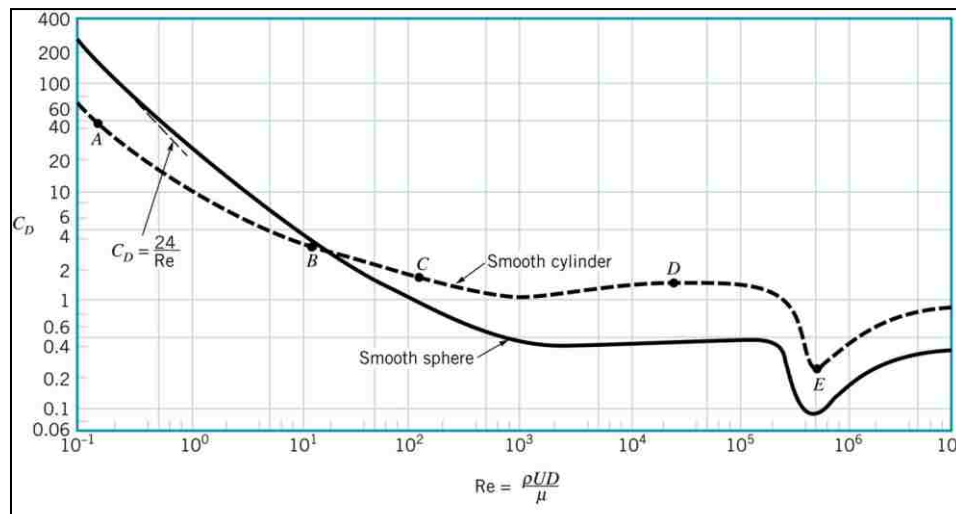


Figure 3. Drag coefficients for a smooth cylinder and sphere as a function of particle Re (Munson et al. 2012)

Another important consideration when studying the interactions of flow and vegetation is the fact that most vegetation elements are highly deformable. Vegetation will bend and streamline when exposed to a velocity field. Vollsinger *et al.* (2005) investigated plant deformation in the form of the crown's changing projected area. The authors developed species and leaf-condition specific curves to relate the vegetation's initial area of interception with its streamlined area. Freeman *et al.* (2000) conducted flume experiments on dozens of specimens in order to investigate drag forces as a function of approach velocity. In an interesting result, the drag force was found to have a nearly linear relationship with approach velocity. In other words, the streamlining reduced the expected drag force in a way that the drag force was linearly related to velocity rather than exponentially as we would expect from theory.

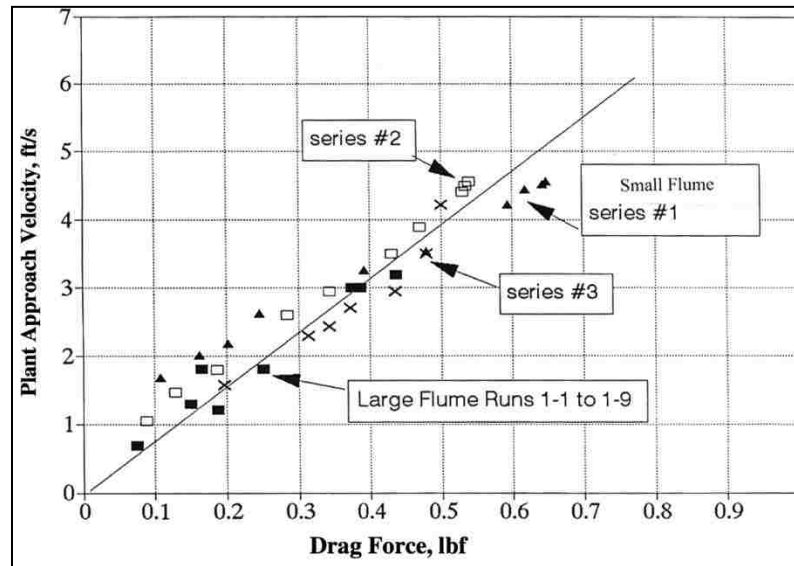


Figure 4. Plant drag force as a function of approach velocity (Freeman et al. 2000)

Numerous attempts (e.g. Kouwen 1973; Thompson and Roberson 1976; Jarvela 2004) have been made to quantify vegetation induced roughness in river and stream

systems, and these attempts have ranged from highly theoretical (e.g. Thompson and Roberson 1976) to highly empirical (e.g. Jarvela 2004). A summary of the five most highly cited techniques is provided in Table 1 below and additional information regarding the application of these techniques is provided in Appendix A. In these roughness calculation approaches, all formulae use some representation of vegetation density (e.g. $m \cdot D$ for Baptist 2007; LAI for Jarvela 2004) and some version of a drag coefficient. Some of the techniques have been formulated to directly account for vegetation deformations. Other formulas have the capability to account for stem deformation indirectly by adjusting the effective density and/or drag coefficient (e.g. Jarvela 2004). Practically all of these methods have only been validated in laboratory settings. Further, investigations of the approaches for computing roughness parameters in the field are rare and no studies exist in the referred literature investigating uncertainty in the various approaches.

Table 1. Summary of common methods for estimating vegetation roughness

| Approach | Formula | Definition of input variables |
|------------------------------|---|--|
| Thompson and Roberson (1976) | $\frac{U}{U_o} = 0.48 \left(\frac{S_v}{d_v} \right)^{0.14}, 4 \leq \left(\frac{S_v}{d_v} \right) \leq 20$ $\frac{U}{U_o} = 0.70 \left(\frac{S_v}{d_v} \right)^{0.08}, 20 \leq \left(\frac{S_v}{d_v} \right) \leq 100$ | <p>U = Mean velocity (m/s) U_o = Approach velocity (m/s) S_v = Stem spacing (m) d_v = Stem diameter (m)</p> |
| Kouwen and Li (1980) | $MEI = \left[3.4h \left(\frac{k}{h} \right)^{0.63} \right]^4 (\gamma y_n S_f)$ $k = 0.14h \left[\frac{\left(\frac{MEI}{\gamma y_n S_f} \right)^{0.23}}{h} \right]^{1.59}$ | <p>MEI = Vegetative stiffness k = Deflected stem height (m) h = Original stem height (m) S_f = Friction slope Y_n = Normal flow depth (m) γ = Water specific weight (N/m³)</p> |
| Kouwen and Fathi (2000) | $f = 4.06 \left[\frac{U}{\sqrt{\frac{\xi E}{\rho}}} \right]^{-0.46} \left(\frac{y_n}{h} \right), \text{ For } y_n \leq h$ $f = 6.17 \left[\frac{8gRS_f}{\xi E / \rho} \right]^{-0.3}$ | <p>ξE = Vegetation index see (Gathi (1996)) f = Darcy-Weisbach coefficient</p> |
| Jarvela (2004) | $f = 4C_{dr}LAI \left(\frac{U}{U_r} \right)^{-r_f} \frac{h}{H}$ | <p>LAI = Leaf area index C_{dr} = Species-specific coefficient r_f = Species-specific exponent U_r = Referenced velocity (1.0 m/s) h/H = 1</p> |

| | | |
|-------------------|---|--|
| Baptist (2007) | $\tau_t = \rho g h S_f$ $\tau_b = \rho \frac{U^2}{C_b^2}$ $\tau_v = \frac{1}{2} \rho C_D m D h U^2$ | τ_t = Total shear stress τ_v = Stems roughness drag coefficient τ_b = Stream bed roughness drag coefficient g = Acceleration due to gravity ($m^3 \text{ kg}^{-1} \text{ s}^{-2}$) ρ = Flow density (kg/m^3) C_b = Steam bed Chezy coefficient C_D = Bulk drag coefficient m = # of stems per m^2 (m^{-1}) D = Stem diameter (m) |
|-------------------|---|--|

Methods

A combination of analytical and experimental approaches was used to address the study objectives. A spreadsheet calculator was developed to easily investigate the five vegetation roughness calculation approaches summarized in Table 1. Two of the approaches (Thompson & Roberson and Jarvela) were further investigated using MATLAB in order to more fully investigate the role of parameter uncertainty on roughness and depth estimates. The uncertainty assessment was performed using the San Luis Rey in Oceanside, California as a test case. Finally, an experimental flume was constructed in order to investigate turbulence characteristics in the presence of artificial vegetation elements. The measurements are intended as a first step towards a more physically based predictive method for vegetation roughness.

Roughness Calculator Spreadsheet

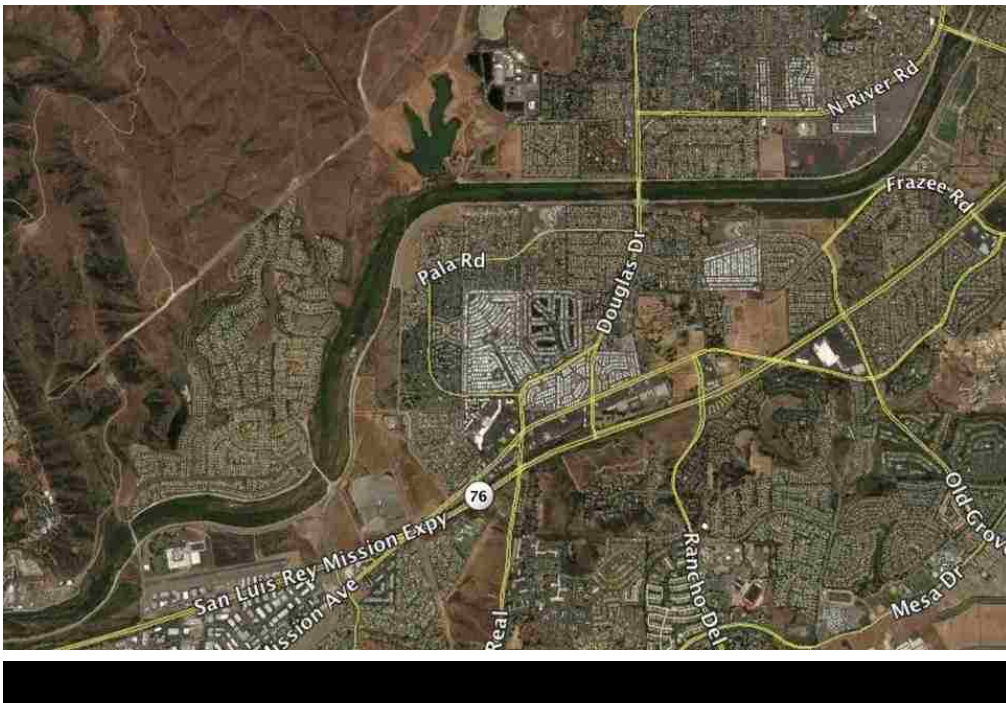
A Roughness Calculator spreadsheet was developed using Microsoft Excel to aid in computing hydraulic roughness in open channel flows with emergent vegetation canopies. The spreadsheet is intended to provide the user with a rapid and easily applied tool for assessing vegetation roughness. The spreadsheet contains roughness estimation functions from equations including the evaluation of Manning's n proposed in studies

done by Thomson and Roberson (1976), Kouwen and Fathi (2000), Kouwen and Li (1980), Jarvela (2004) and Baptist *et al.* 2007 (Table 1). These methods were compiled in order to effectively perform input parameters sensitivity assessments and quickly evaluate their subsequent impacts on results. The interface of the roughness spreadsheet shows four (4) main types of cells. The required input parameters are recorded in yellow cells, the simulation output results figure in green cells, the results of interest (i.e. Manning's n and Darcy-Weisbach, f) are output in blue cells, and the calculation error estimate is shown in a red cell. Although some of the methods are a bit similar in terms of their general input parameters (i.e. vegetation characteristics), they still produced results that were significantly different from one method to the next. Within this study, the spreadsheet calculator was used to perform a simple sensitivity study. Input parameters were varied one at a time and the corresponding impacts on the output variables (primarily Manning's n) were systematically investigated.

Uncertainty Assessment

Results of the sensitivity assessment revealed a relatively large degree of sensitivity to changes in the parameters that represented vegetation density and drag. Thus, a more sophisticated uncertainty analysis was performed using the Jarvela (2004) and Baptist *et al.* (2007) approaches. These two techniques were selected because the researchers had access to parameterization data for a test site – the San Luis Rey River (SLR). The SLR is located in southern California, 150 km south of the City of Los Angeles and 50 km north of San Diego in San Diego County, California. The U.S. Army Corps of Engineers (USACE) implemented a substantial flood risk reduction project on the SLR in the late 1980s. The project encompassed a total of 12 km along the river and

included significant channelization and construction of massive levees (Figure 5). The goal of the original SLR flood risk reduction project was to control flow depth and extent to a safer level in the event of floods in order to encourage floodplain development. The designed flow depth was between 5.5 to 6.4 m. To achieve these numbers, design engineers targeted vegetation and sediment removal as they were the most controllable physical inputs beyond channel geometry.



Congress authorized a plan for flood control, which was designed and constructed to convey a standard project flood of $2,500 \text{ m}^3/\text{s}$ (89,000 cfs), but due to lack of continuous maintenance of the channel, the flow conveyance has dropped to approximately $1,330 \text{ m}^3/\text{s}$ (47,000 cfs). The unmanaged vegetation has become home to two species of



endangered birds (the bell's vireo (*Vireo bellii*) and southwestern willow flycatcher (*Empidonax traillii extimus*)) and thus the USACE is no longer able to conduct vegetation removal as proposed in the original design (Figure 6). Thus, the USACE and the U.S. Fish and Wildlife Service (USFWS) are seeking a management plan to protect endangered species while increasing channel conveyance. The proposed actions include vegetation management (i.e. removal of bushes and shrubs) and sediment removal. Upon implementation of these actions, it is believed that the channel conveyance will be increased to approximately 2,010 m³/s (71,000 cfs).

In this study, the application of the Jarvela (2004) and Baptist *et al.* (2007) vegetation roughness algorithms were tested using data from the SLR. The uncertainty of the two approaches was investigated using a Monte Carlo approach within MATLAB. Input parameters were allowed to vary within specified distributions in order to evaluate the range of output conditions. Because the details of the input parameter distributions are not known, two distribution types were tested. First a uniform distribution was specified for all input parameters with ranges derived from the literature. Second, normal distributions were specified with means and standard deviations again derived from literature values.

Laboratory Investigation

An experimental flume (1 meter by 6 meter) was constructed in the Hydraulics Lab in the UNM Civil Engineering Department (Figure 7). The flume was constructed with a stainless steel bed in order to allow us to easily affix and remove artificial vegetative elements using magnets (Figure 3). 3D velocity components were recorded with a 3D Acoustic Doppler Velocimeter (ADV) (Figure 8) mounted on platform placed

on top of the flume walls. The water surface within the flume was monitored upstream and downstream of the test section using a point gauge. The channel slope and the water surface slope were measured with a total station.

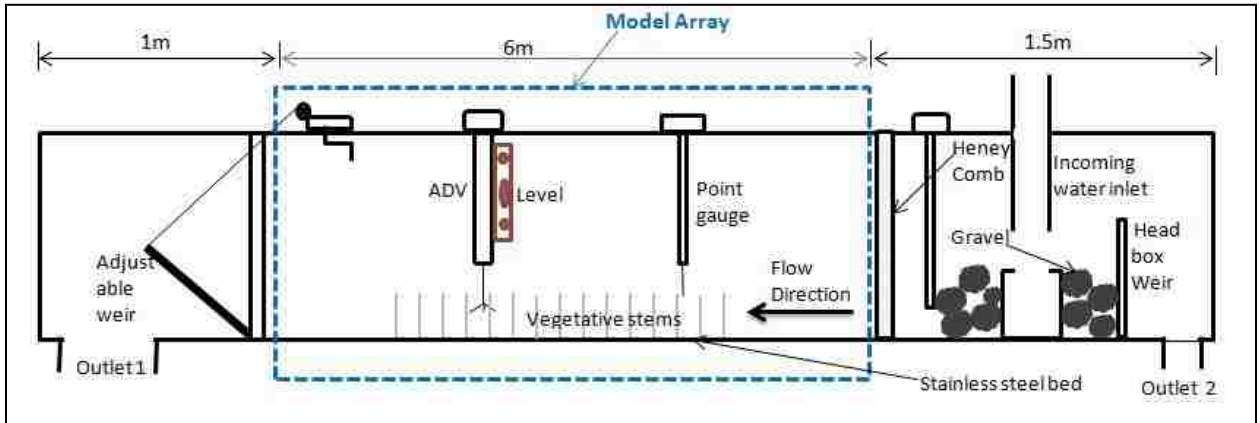


Figure 7. Schematic of a profile view of the experimental flume



Prior to placing vegetation canopy in the flume, flow characteristics were taken within the flume without vegetation as a control. The flume was run for several hours until the flow became uniform and steady. Velocity profiles were taken in various areas of the flume (i.e. streamwise, spanwise, and vertical channel profiles)



upstream, within, and downstream of the artificial

vegetation canopy. Data was collected for two-minutes at 25 Hz at every station. The ADV was positioned within the canopy with little or no disturbance to the array configuration (i.e. displacing the stem dowels). The cylindrical plastic vegetative stem heights were 15 cm tall with each having diameter of 2.5 cm.

The ADV produces time series (25 Hz) of the 3D velocity vector. In order to process this information, a MATLAB script was written to calculate mean and statistical

characteristics of the flow including turbulent kinetic energy (TKE), integral time scale (T), and integral length scale (L) (See Appendix D for code). The description of flow fields can be separated into mean velocity and turbulent fluctuations. Mean velocity is typically time-averaged at a point in the flow field. Turbulence can be investigated statistically as velocity fluctuations at a point or through the study of coherent structures. The physical implication of mean velocity and turbulent fluctuations is the transfer of mass, momentum, and energy through the flow field.

The separation of flow descriptions into mean and turbulent features is formalized through the Reynolds decomposition (Reynolds 1974):

$$u_i^{\zeta} = u_i - \bar{u}_i$$

where u_i^{ζ} , u_i , and \bar{u}_i denote the fluctuating, instantaneous, and time averaged velocities in each coordinate direction, respectively. The fluctuating velocity components are evaluated through statistical techniques. A common evaluation parameter for turbulent velocity fluctuations is the turbulent kinetic energy (TKE). TKE is analogous to mean kinetic energy and is calculated as:

$$TKE = \frac{\overline{u_i u_i}}{2}$$

where $u_i u_i$ is the sum of the squared velocity fluctuations in each coordinate direction. TKE can be used to study the flow field energy budget and is an important parameter in turbulence modeling.

More information about the turbulent features of the flow field can be gained through investigation of coherent structures. This is accomplished by calculating time and length scales. Time scales can be determined through investigation of auto-correlation functions. Auto-correlation functions are derived by calculating the correlation of the

time series with itself at an increasing level of lag interval in order to produce an auto-correlation term as a function of lag time ($R(t)$). The average persistence of turbulent activity at a point is the integral time scale and it is calculated by integrating the auto-correlation function as:

$$T = \int_0^{t_R} R(t) dt$$

where T is the integral time scale and t_R is the correlation time. t_R is defined as the time at which the correlation function goes to zero.

Length scales can be used to measure the average spatial extent of the velocity fluctuations. Integral length scales can be calculated from integral time scales using Taylor's Frozen Turbulence Hypothesis as follows:

$$L = \bar{u}_s T$$

where L is the integral length scale, and \bar{u}_s is the mean streamwise velocity. Taylor's hypothesis has been confirmed valid in open channel flows for relative depths greater than 20% (Steinman et al. 1996).

Results

The objective of this research was to evaluate methods for determining hydraulic roughness within open channels in the presence of vegetation and to advance understanding of the influence of vegetation on turbulence characteristics of flow. Out of the five methods investigated here, two approaches (Jarvela 2004 and Baptist *et al.* 2007) were proven to be more applicable to the real-world open channel conditions whereas the remaining three models simulations required data that is difficult to contain and apply in a practical manner. Thus, the Jarvela and Baptist approaches were selected for closer investigation via an uncertainty assessment for a test case. Finally, flume experiments

were used to more carefully investigate the mechanisms of energy dissipation and general fluid dynamics using artificial vegetation.

The Roughness Calculator spreadsheet was used to perform a sensitivity analysis by varying input parameters such as vegetation index (ξE), LAI, and vegetation density. The results from the models showed a notable sensitivity of Manning's n values to the various input parameters. The variation in results due to LAI could be physically explained because LAI is a direct reflection of vegetation density, which largely induces the bulk vegetation impact on the water flow within the channel. The parameters m and D in Baptist method were treated as single composite parameter and the sensitivity analysis showed that the approach is fairly sensitive to vegetation density coupled with stem diameter. Figures 9 and 10 provide examples of sensitivity test outputs for the Jarvela and Baptist approaches, respectively. In Figure 9, the LAI is varied from 0.5 to 3.5 (typical range of field values) as the Jarvela specific drag term (C_{dr}) was varied from 0.4 to 0.7. Manning's n varied noticeably as a function of these input variables. For example, based on the same LAI, the resulting Manning's n varied by as much as 25% as C_{dr} was changed from 0.4 to 0.7. Manning's n varied by nearly 2-fold as LAI was increased from 0.5 to 3.5. The trends were as expected and the range of variability was consistent with expectations based on the underlying equations and team's knowledge of these systems.

The Baptist predictions were overall less sensitive to input parameters, but still showed marked variation across the range of tested values. Variation in Manning's n as a function of the C_d was observed to be relatively mild, which is an important finding considering the difficulty in selecting in a representative C_d . Manning's n was found to be highly sensitive to the vegetation density function ($m \cdot D$) at low values but relatively insensitive at $m \cdot D$ values above 1. This also has important implications for application

studies and suggests more care should be given to collecting density data when the vegetation is relatively sparse. Sensitivity of the remaining three approaches was also investigated. However, the results are not included here because the research team has a low degree of confidence in the estimated range of input data. Similar trends were observed for all five approaches.

It should also be noted that the predicted Manning's n values based on the Baptist approach were noticeably higher for the Baptist approach when compared with the Jarvela method. The range of input values for each technique was used with intention to reflect similar vegetation conditions based on the researchers' experience.

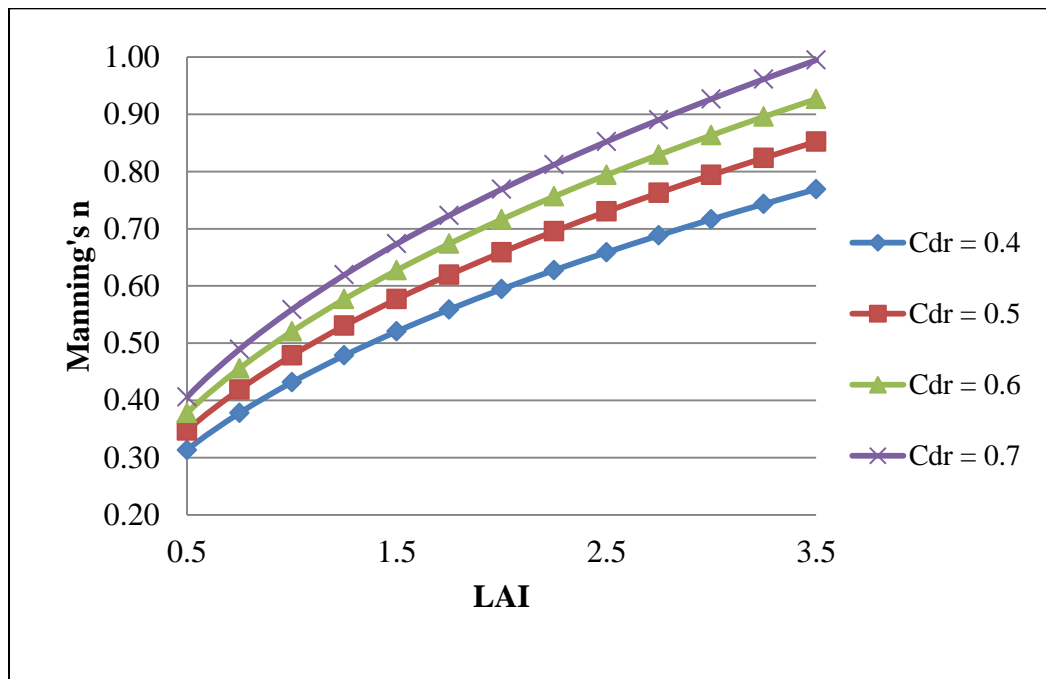


Figure 9. Variation in Manning's n as a function of LAI and C_{dr} based on Jarvela (2004)

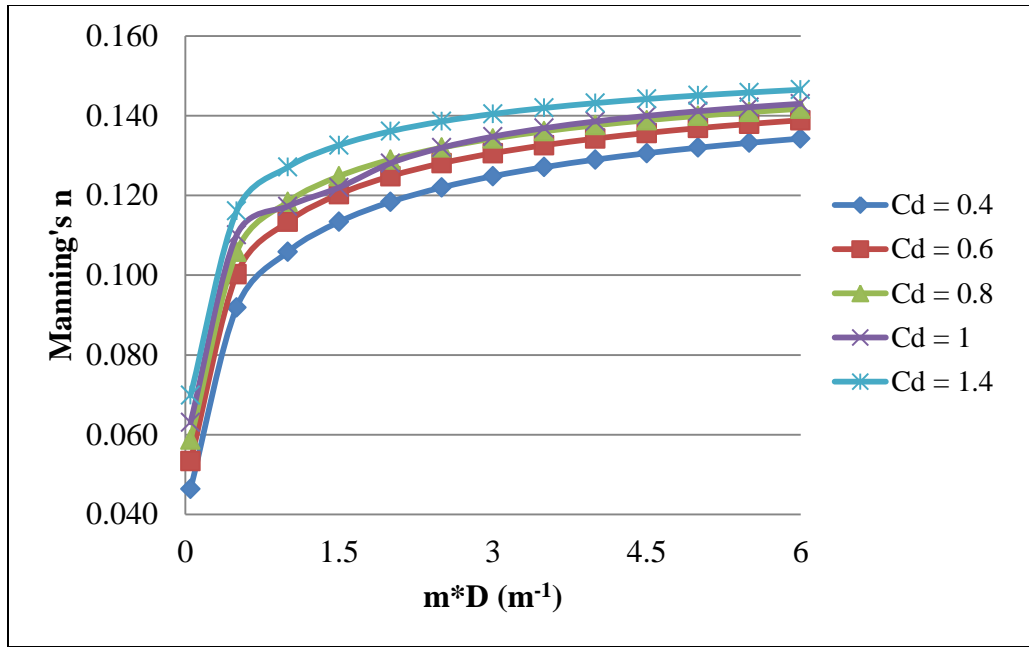


Figure 10. Variation in Manning's n as a function of vegetation density and C_d based on Baptist et al. (2007)

Following the sensitivity analysis, a more robust investigation of uncertainty was carried out by conducting a Monte Carlo based simulation of the Jarvela and Baptist approaches. In order to provide context and to help in selecting a realistic range of input data, the uncertainty analysis was conducted on the SLR project reach using vegetation data collected by Goreham (2009). The Monte Carlo simulation was completed with MATLAB (see Appendix C for full code). For both methods, 10,000 simulations were conducted where Manning's n was calculated using both techniques and the normal water surface depth (y_n) was calculated using a typical SLR cross-section and the Manning's equation. Input values for the parameters C_{dr} and X for Jarvela and for C_d for Baptist were allowed to vary across the ranges reported in the literature. Input values for LAI and $m \cdot D$ were specified by the user and are considered to represent different scenarios of vegetation clearing. LAI was varied from 0.25 to 1.0 and $m \cdot D$ was set between 0.05 to 1.5.

Raw output from the Monte Carlo simulations are shown in Figures 11 and 12 for the Jarvela and Baptist approaches, respectively. Histograms representing the frequency of Manning's n values are presented for two different input (vegetation) conditions. Further, the results are presented for two different prior distributions for input parameters: uniform (left column) and normal (right column). The results indicate a wide range of variability for predicting Manning's n based on both approaches. In both cases, the variability was higher for the uniform input distributions when compared with the normal input distributions. Again, the Manning's n values determined using the Jarvela approach were noticeably higher than those calculated with the Baptist method. As was the case in the sensitivity analysis, the roughness also varied a great deal more based on the Jarvela approach than it did using the Baptist approach.

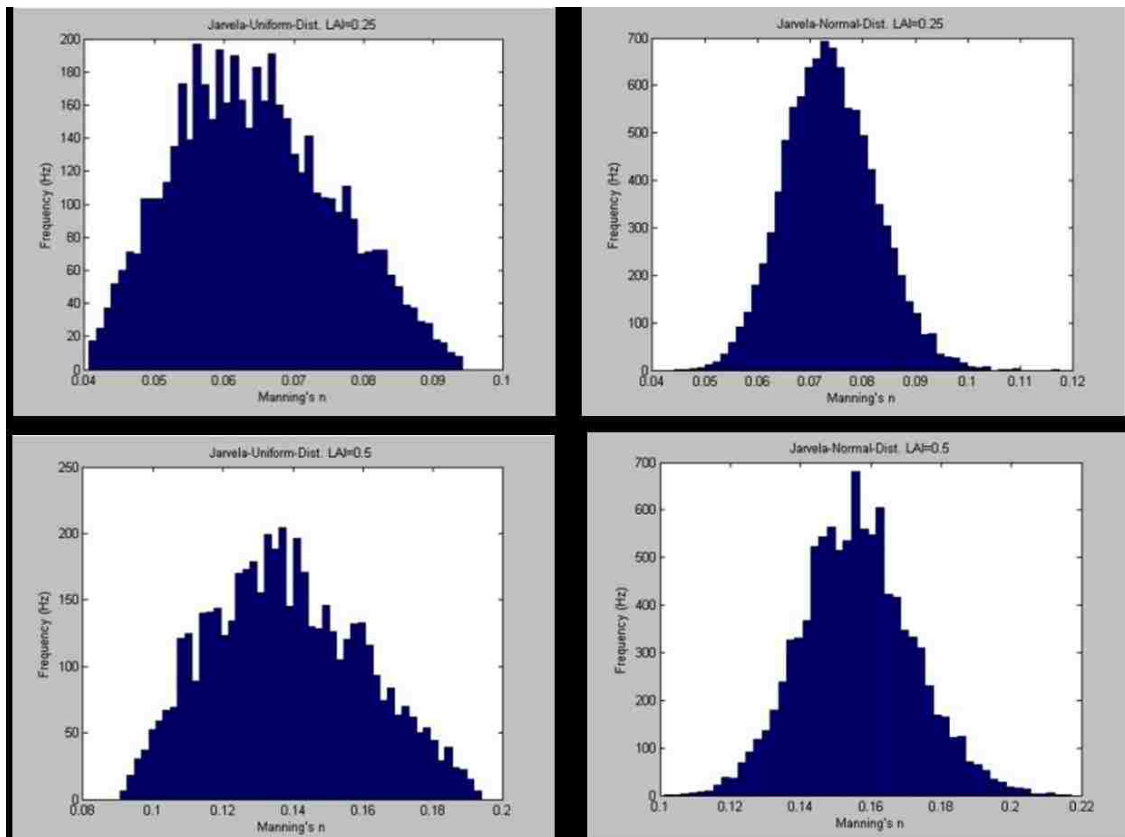


Figure 11. Histogram for the Jarvela approach.

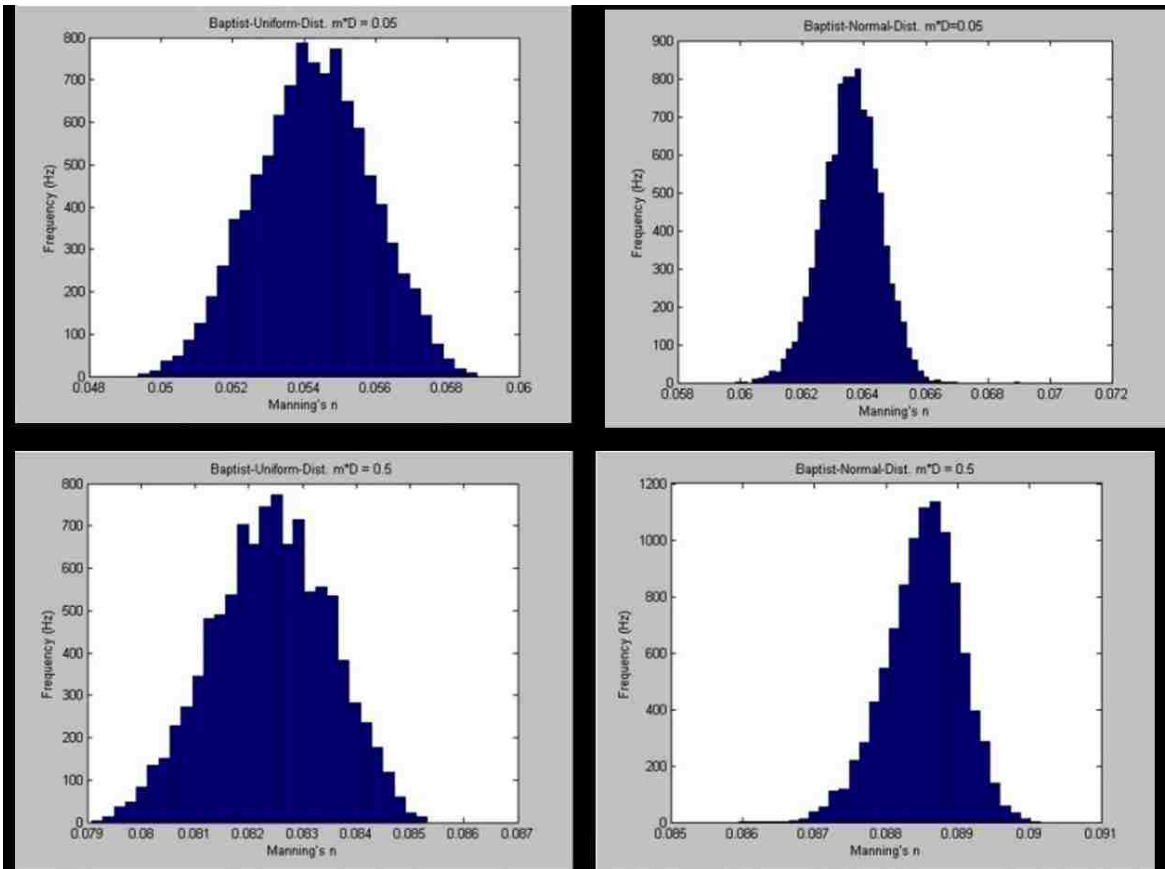


Figure 12. Histogram for the Baptist '07 approach.

In order to more clearly investigate the results of the sensitivity analysis, the mean and standard deviation for each output distribution from Monte Carlo simulations were calculated. The results for Manning's n and y_n from the Jarvela approach are shown in Figures 13 and 14 and for the Baptist approach in Figures 15 and 16. Several notable trends are observed. First for the Jarvela method, it's obvious that the results are highly dependent on the selected LAI value. Within a selected LAI value the variability, represented by the standard deviation, is high. The approach is less sensitive when considering the output distributions for y_n . As for the Baptist approach, the method is less dependent on the density function (as compared to LAI for Jarvela). As reported from the sensitivity analysis, the sensitivity to $m*D$ is higher at the lower end of the scale. However, the level of variability within a given density value was only slightly less than

that for Jarvela for a given LAI value. Overall, the predicted Manning's n and y_n values were higher for the Jarvela method than for the Baptist approach.

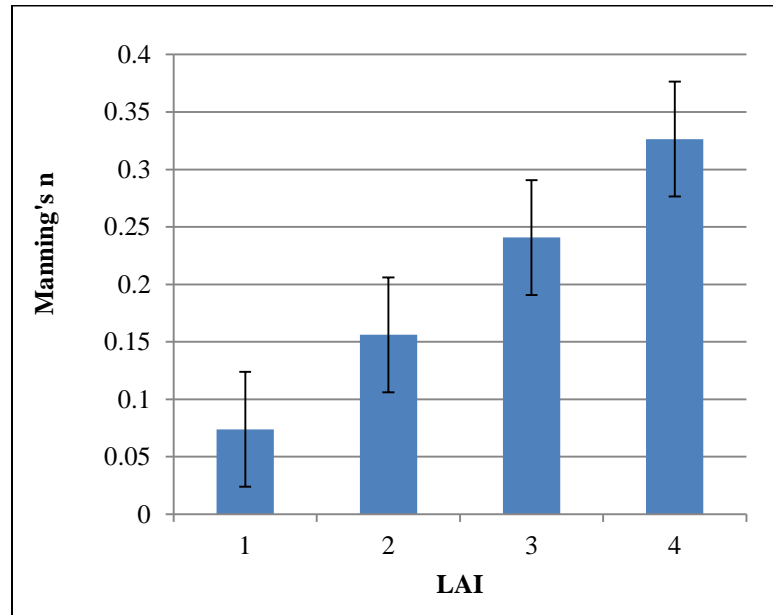


Figure 13. Jarvela '04 approach, Manning's n as function of LAI

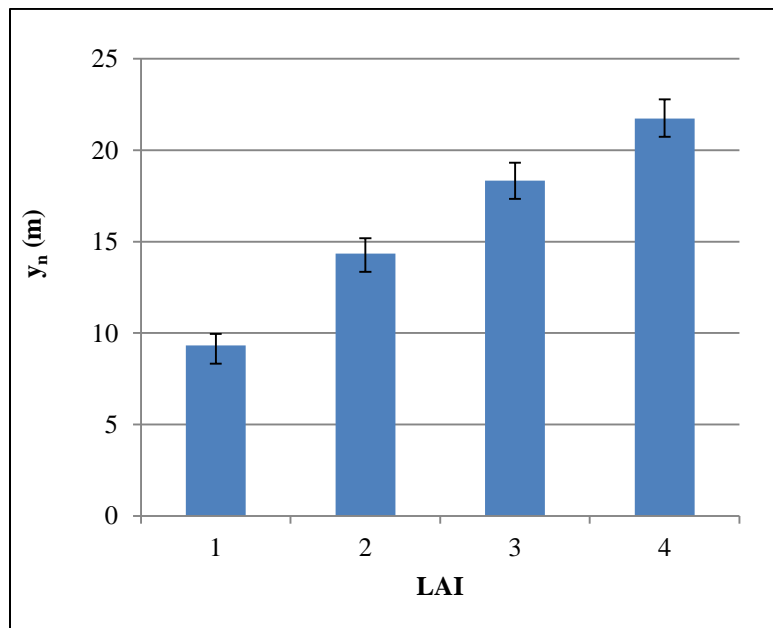


Figure 14. Jarvela '04 approach, normal depth as function of LAI

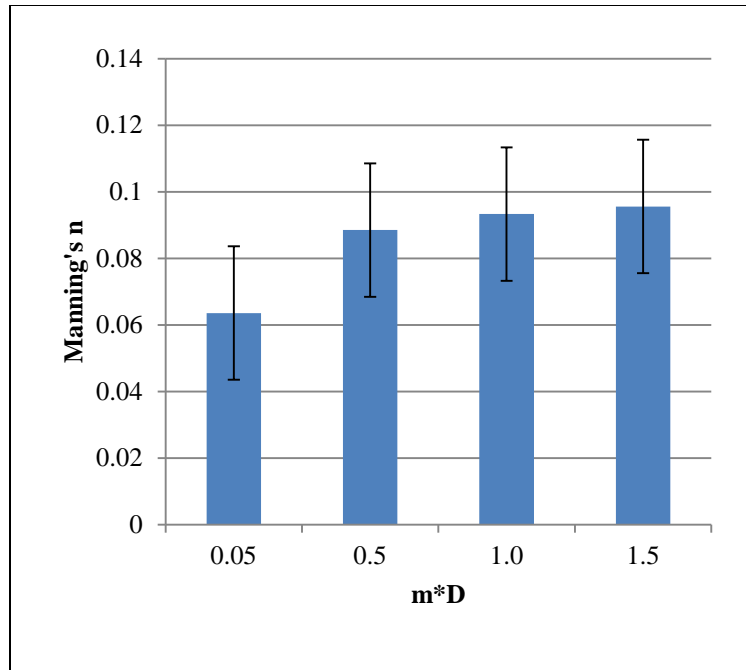


Figure 15. Baptist '07 approach, Manning's n as function of m*D

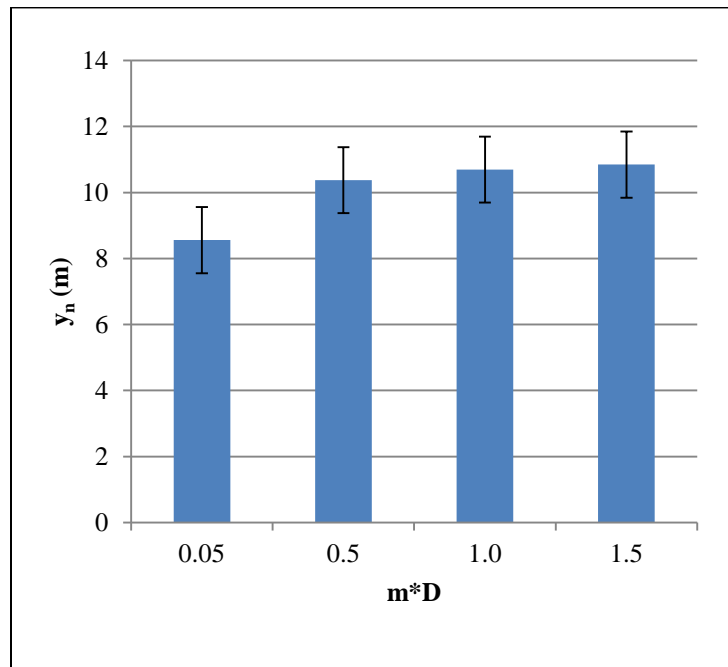


Figure 16. Baptist '07 approach, normal depth as function of m*D

Turbulence characteristics were evaluated using ADV measurements at three stations (upstream, mid-canopy, and downstream) under four flow conditions, which are described with respect to the approach velocity. Three metrics were selected to describe

the influence of artificial vegetation elements on the energy budget (TKE) of the flow field along with the turbulence structure (L and T). Data was collected at six locations at each cross-section.

TKE results are included in Figure 17 at all three stations and four flow conditions. As expected, TKE values were lowest at the upstream station and lowest within the canopy with intermediate values downstream. Upstream, the mechanism for TKE generation is limited to shear stress with the bed driven by gravity. Within the canopy, however, significant TKE is generated within the wake regions of each vegetation element. This process represents the transfer of energy from the bulk flow (kinetic energy) to turbulent elements (TKE) in the form of small scale vortices. This energy is ultimately lost to viscosity in the form of heat. TKE also varied within a region in that it generally increased as a function of velocity.

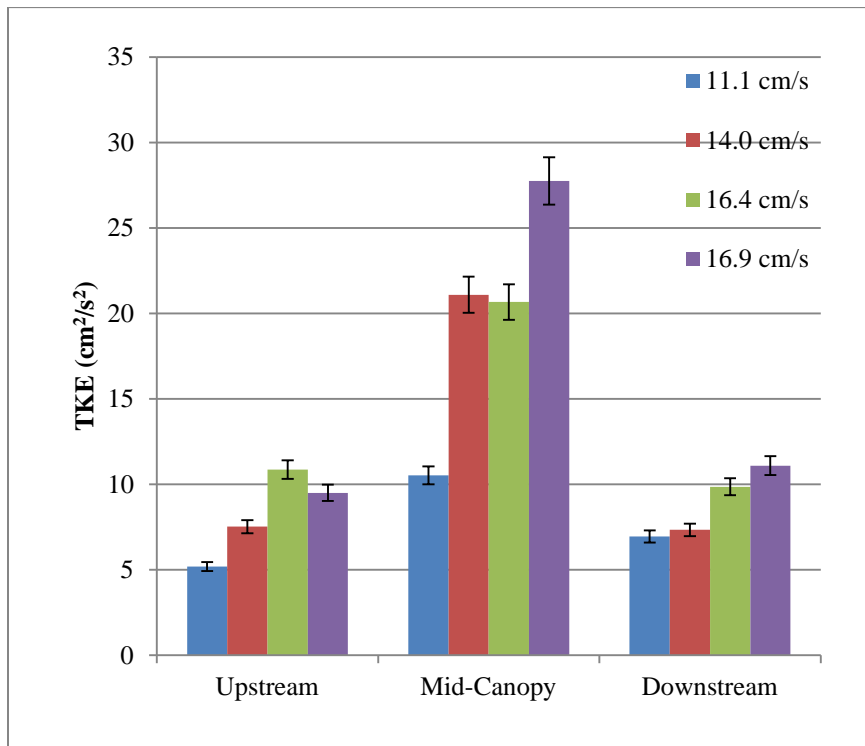


Figure 17. Turbulent kinetic energy (TKE) as a function of location and approach velocity

Integral length scales and integral time scales are summarized in Figures 18 and 19, respectively. For both metrics, the scale was reversed from that of TKE. That is the length and time scales were highest upstream of the artificial vegetation and lowest within the canopy. Upstream from the canopy, turbulence scales (eddy size) was limited by the geometry of the flume. Consequently, the length scale was commensurate with the flow depth of approximately 11 cm. As the flow entered the vegetation canopy, the eddies were rapidly broken down to a much smaller scale. Further, smaller eddies were produced in the wake of the vegetation elements (expected to be of a similar dimension as the elements). As a result, both integral length and time scales dropped drastically within the canopy. Finally, the scales began to recover and increase downstream from the canopy. Within a station, the results were moderately sensitive to the approach velocity. Upstream, the length scale increased slightly with velocity – likely caused by more energy available for building vortices. However, within the canopy, scales actually decreased with velocity. We speculate this is because additional small-scale vortices were being produced due to greater energy availability. This however, is worthy of further investigation.

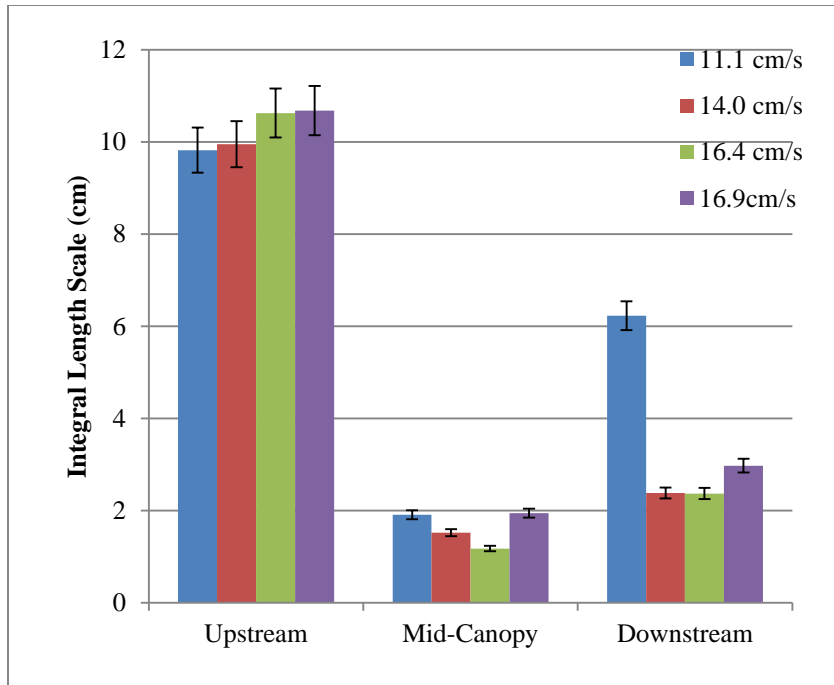


Figure 18. Integral length scale (L) as a function of location and approach velocity

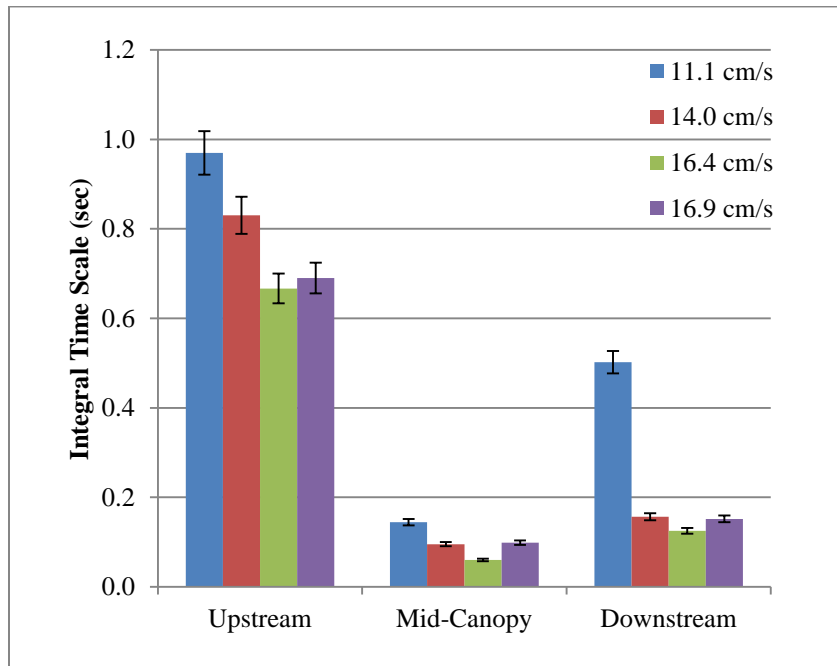


Figure 19. Integral time scale (T) as a function of location and approach velocity

Discussion

Hydraulic roughness in the presence of vegetation is notoriously difficult to predict. However, reliable methods for predicting flow resistance in vegetated channels

and floodplains are needed in order to address the needs of modern river engineering. To this end, the objectives of this research were: (1) to evaluate methods for determining hydraulic roughness within open channels in the presence of vegetation, and (2) to advance understanding of the influence of vegetation on the turbulence characteristics of the flow field.

This research investigated five approaches for estimating roughness, which have emerged in the literature over the past 36 years. Each of these approaches aims to produce a roughness value, but the underlying approaches, assumptions, data requirements, and sensitivities vary greatly between the methods. All of the techniques, however, rely upon some representation of vegetation density, structure, and species specific drag coefficient. Working with these techniques revealed the relative strengths and weaknesses of the various approaches. This work revealed that two of the techniques (Jarvela and Baptist) proved to have a better utility than the others with respect to the availability of input data, suggestions for parameterization, and ease of application. Thus, these two approaches were used much more extensively within this research while the remaining three approaches were discarded because they failed to converge during the mathematical simulation in the roughness spreadsheet.

A sensitivity analyses showed that both the Jarvela and Baptist approaches were sensitive to inputs (i.e. species-specific drag coefficients, stem spacing, stem diameter, LAI, etc.) as the output values varied markedly. The variability in output results can be attributed to the assumptions within the approaches and the lack of species and location specific input data. An example of a major underlying assumption is that Baptist assumes the vegetative elements are perfectly cylindrical and are geometrically arranged in gridded or staggered fashion. Further, they assume the distribution of bulk vegetation

density to be homogeneous throughout the channel, which is seldom the case in natural stream systems.

Another significant assumption with respect to application of these techniques lies in the engineer's ability to obtain accurate and reliable data to input into the techniques. Drag coefficients cannot be determined by a practitioner because it requires large, complex, and expensive equipment. However, published data are only available for a small number of species and conditions. Further, the methods require input data that are tedious to collect and highly heterogeneous in the field. For example, an enormous amount of effort (i.e. Ground based LiDAR) is required to characterize the number, spacing, and diameter of stems.

The Monte Carlo based uncertainty assessment provided additional insights of how uncertainty within the input data propagates through to uncertainty in predictions of hydraulic roughness and water depth. Overall, the assessment revealed a fairly high degree of uncertainty that depended on assumptions made when specifying the input parameters including the type of prior distribution (uniform vs. normal). We can conclude from this exercise that the input variability must be reduced in order to have confidence in the results produced by these methods. This could be accomplished by increasing the database of species specific parameters. This is not practical to perform on a case by case basis and thus it is recommended that a systematic and extensive study be carried out by the USACE, FEMA, or other related federal agency.

With respect to the SLR case study, the results were highly dependent on the method (Jarvela or Baptist) and the assumptions regarding vegetation density. For example, the predicted normal depth jumped from 10 m to approximately 18 m when adjusting LAI from 1 to 3.5. The results revealed that it is highly unlikely that the flood

risk reduction study will be capable of safely conveying the design discharge – even under fairly aggressive vegetation removal schemes. Although this is not an encouraging result, it does provide the USACE with a more advanced understanding of the condition they are facing and allows them to begin appropriate planning. The conclusions here are not dissimilar from USACE’s previous findings, but the incorporation of uncertainty provides a much more robust perspective than that provided by USACE’s previously conducted deterministic study.

Finally, the investigation of turbulence metrics within a flume study is an important first step for improving understanding basic fluid dynamics in the presence of vegetation. Several interesting trends emerged from the flume experiment that can be used to guide future research in this area. TKE values increased substantially as the flow passed through the artificial vegetation. Although not performed here, it could be possible to integrate the TKE production through the vegetation canopy in order to quantify how much energy is being transferred from bulk KE to TKE. The reduction in length scales from a value similar to the flow depth, upstream of the vegetation, to that similar to the vegetation elements, within the vegetation, provided very intriguing insights to how the vegetation is influencing the turbulence structure. Future work in this area should focus on describing the turbulence spectral characteristics within the vegetation and the process in which the vegetation serves to “short-circuit” the turbulence energy cascade.

Conclusion

The research discussed in this thesis provides important steps forward in two specific ways when considering the prediction of hydraulic roughness and water depths in the presence of vegetation. The two areas include an improved understanding of the

utility of commonly cited vegetation roughness routines and the influence of vegetation on turbulence characteristics. We conclude the following:

- (1) Of the various methods available for estimating hydraulic roughness in the presence of vegetation, two approaches showed the most promise with respect to data availability and ease of application – Jarvela (2004) and Baptist et al. (2007).
- (2) All of the hydraulic roughness estimating techniques showed a high degree of sensitivity to input parameters including descriptions of vegetation density and drag coefficients.
- (3) Uncertainty in input parameters translates to uncertainties in predictions of hydraulic roughness and flow depth. Thus, future research should aim to improve species specific estimates of common parameters and techniques for measuring field parameters.
- (4) A case study on the SLR revealed that even within the range of uncertainty, existing proposals to remove channel vegetation are unlikely to result in channel conveyance at the level intended in the original appropriation for the flood risk reduction study.
- (5) Turbulence metrics can provide much insight into the mechanisms in which energy is extracted from the bulk flow as a result of drag forces. This area of research shows promise with respect to developing general models for predicting hydraulic roughness.

Future Research

In spite of significant research on the topic, much research is still needed before consistent, general, and easily applied techniques will be available for predicting channel roughness in the presence of vegetation. Due to the high degree of sensitivity and

uncertainty in the roughness predictions resulting from uncertainty in input variables, future work should focus on improving species specific estimates of input data (i.e. χ , C_{dx} , ξE). This represents an enormous undertaking, however, it is important information for reducing uncertainty, which in the end can reduce project expenses or property losses due to poor designs. The turbulence investigation revealed several interesting trends worthy of future research that ultimately will improve basic understanding of vegetation/fluid interactions and the hydrodynamic models used to describe them.

Literature Cited

- Aberle J., Jarvela J., (2013). "Flow resistance of emergent rigid and flexible floodplain vegetation", *Journal of Hydraulic Res.* Vol.51, No. 1 (2013), 33-45
- Babaeyan-Koopaei, K., D. A. Ervine, P. A. Carling, Z. Cao (2002), "Velocity and Turbulence measurements for two overbank flow events in River Severn", *Journal of Hydraulic Eng.*, 128(10), 891-900, doi: 10.1061/(ASCE)0733-9429(2002)128:10(891)
- Baptist, M.J., (2007). "On inducing equations for vegetation resistance", *Journal of Hydraulic Research*, Vol. 45, No. 4, 435-450.
- Cowan, W. (1956). "Estimating Hydraulic Roughness Coefficients" *Agricultural Engineering*, 37 (7), 473-475
- Freeman, G. E., Rahmeyer, W. H. and Copeland, R. R. (2000). "Determination of Resistance Due to Shrubs and Woody Vegetation". U.S. Army Corps of Engineers. 62p.: ill. , 28 cm.—(ERDC/CHL , TR-00-25)
- Goreham, J.O. (2009). "Bending of woody riparian vegetation as a function of hydraulic flow conditions". Master's thesis, University of Nevada, Las Vegas.
- Guardo, M., and Tomasello, R. S. (1995). "Hydrodynamic Simulations Of a Constructed Wetland In South Florida." *Water Resources Bulletin*, 31(4), 687-701.
- Jadhav, R. S., and Buchberger, S. G. (1995). "Effects of vegetation on flow through free water surface wetlands." *Ecological Engineering*, 5(4), 481-496.
- Jarvela, J., (2004), "Determinatin of flow resistance caused by non-submerged woody vegetation", *Intl. J. River Basin Management* Vol. 2, No. 1, 61-70
- Kadlec, R. H. (1990). "Overland-flow In Wetlands - Vegetation Resistance." *Journal of Hydraulic Engineering-ASCE*, 116(5), 691-706.
- Kadlec, R. H. (1995). "Overview: Surface flow constructed wetlands." *Water Science And Technology*, 32(3), 1-12.
- Kouwen, N. and Fathi-Moghadam, M., (2000), "Friction factors for coniferous trees along rivers", *Journal of hydraulic engineering*, Vol. 126, No. 10, 732-740.
- Kouwen, N. and Ruth-Ming Li, (1980), "Biomechanics of vegetative channel linings", *Journal of the hydraulics division, Proceedings of the American Society of Civil Engineers*, Vol. 106, No HY6, 1085-1103
- Krugman, P. (1998). "What's New about the New Economic Geography?" *Oxford Review of Economic Policy*, 14(2), 7-17.
- Li, R.M. and Shen, H.W. (1973). "Effect of Tall Vegetation on Flow and Sediment". *Journal of Hydraulics Div.* No. 99 (Hy6), 1085-1103.
- Lightbody, A. F. and H. M. Nepf (2006), Prediction of velocity profiles and longitudinal dispersion in emergent salt marsh vegetation. *Environ. Fluid Mech.*, No. 51, 218-228.
- Munson, B. R., Young, D. F., and Okiishi, T. H. (1994). *Fundamentals of fluid mechanics / Bruce R. Munson, Donald F. Young, Theodore H. Okiishi*, New York : Wiley, c1994. 2nd ed.
- Munson, B. R., Young, D. F., & Okiishi, T. H. (2012). *Fundamentals of fluid mechanics / Bruce R. Munson, Donald F. Young, Theodore H. Okiishi*, New York : Wiley, c2012.6th ed.
- Nepf H. M, J. A. S., and R. A. Zavistoski (1997). "A Model for diffusion within emergent vegetation plant canopy." *Limnology and Oceanography*, 42(8), 85-95.
- Nepf H., M. Ghisalberti, B. White, and E. Murphy (2007), "Retention time and dispersion associated with submerged aquatic canopies", *Jounral of Water Resources Research.*, 43, WO4422, doi: 10.1029/2006WR005362.

- Nixon, S. W. (1980). "Between coastal marshes and coastal waters -- a review of twenty years of speculation and research on the role of salt marshes in estuarine productivity and water chemistry." *Estuarine and wetland processes B2 - Estuarine and wetland processes*, Plenum, New York, USA, 438-525.
- Petryk, S., Bosmajian, G. (1975). "Analysis of flow through vegetation", *Journal of the Hydraulics Division, ASCE*, 101 (HY7), 871-884.
- Phillips, J. D. (1989). "Fluvial Sediment Storage In Wetlands." *Water Resources Bulletin*, 25(4), 867-873.
- Rutherford, J. C. (2004), "River Mixing, John Wiley, Chichester, U.K.
- Shi, Z., Pethick, J. S., and Pye, K. (1995). "Flow Structure in and above the Various Heights of a Saltmarsh Canopy: A Laboratory Flume Study." *Journal of Coastal Research*, 11(4), 1204-1209.
- Shucksmith, J. D., Boxall, J. B., and Guymmer, I. (2010). "Effects of emergent and submerged natural vegetation on longitudinal mixing in open channel flow." *Water Resources Research*, 46.
- Thom, A. S. (1971). "Momentum absorption by vegetation". *Quart. J. R. Met. Soc.* (1971), 97, 414-428
- Thompson, G.T. and Roberson, J.A. (1976), "A theory of flow resistance for vegetated channels", *Trans. ASAE*, 19(2), 288-293.

Appendix A-Nomenclature

In this thesis, the symbols used are:

| | |
|---------------------|---|
| A, | Momentum absorbing area or projected area |
| a, | Velocity coefficient |
| b, | Channel bed width |
| C_B , | Chezy coefficient of the stream bed |
| C_D , | Drag coefficient |
| D, | Vegetation diameter |
| d_v , | Vegetation stem diameter |
| Error, | Estimation of error between Q_{measured} and Q_{computed} |
| f, | Darcy-Weisbach friction factor |
| g, | Acceleration due to gravity |
| H, | Flow depth |
| hp, | Vegetation height |
| K, | Units |
| LAI, | Leaf area index |
| MEI, | Vegetation rigidity |
| n, | Manning's n |
| P, | Wetted perimeter of the channel |
| Q, | Flow discharge with the stream |
| Q_{calc} , | Flow discharge computed |
| R, | Hydraulic radius |
| S_f , | Friction slope |
| S_o , | Channel bed slope |
| s_v , | Vegetation spacing |
| U_0 , | Approached velocity |
| U_v , | Velocity within the vegetation |
| y_n , | Flow depth |
| z_1 , | Datum |
| ξ_E , | Vegetation index |
| ρ , | Fluid mass density |
| τ , | Boundary shear stress |

Appendix B - MatLab Code

Baptist et al. (2007) approach

Uniform Distribution code:

```
% Baptist with a Uniform input distribution
% Input Channel Variables
Q1=2520,
b=122,
m=2,
So=0.00125,
nL=0.01,
nH=5,
yL=0.01,
yH=100,

% Input Vegetation Variables (constant parameters set in
baptist.m)
% Cb=100, % Chezy coefficient for the streambed
vd1=5, % Vegetation density, designated as 'm' in Baptist
D1=0.4, % Mean stem diameter

% Vegetation uncertainty loop
nsamples=1000
for i=1:nsamples
    Cd=1.3+rand(1)*0.4,
    CdH(i)=Cd,
    Cb=25+rand(1)*50,
    CbH(i)=Cb,
    vd=(vd1-(vd1/10))+rand(1)*(vd1/5),
    vdH(i)=vd,
    D=(D1-(D1/10))+rand(1)*(D1/5),
    DH(i)=D,
    [ f(i),n(i),y(i),Ck(i) ] =
baptist_bisection(Q1,b,m,So,nL,nH,yL,yH,Cd,Cb,vd,D),
end
    mean(n)
    std(n)
    mean(y)
    std(y)
```

Baptist.m Code:

```
function [Ck,f,nb,resn] = baptist(n1,y,R,Cd,Cb,vd,D)
%Baptist routine
H=0.1; % Mean vegetation height in meters
g=9.81;
Ck=((1/((1.0/(Cb^2))+((Cd*vd*D*H)/(2*g))))^0.5)+((g^0.5)/0.41)*log(y/H);
f=(8*g)/(Ck^2);
nb=1/(Ck*(R^0.1666667));
resn=((nb-n1)/n1)*100;

end
```

Baptist bisection code:

```
function [ fb,nb,yb,Ckb] =
baptist_bisection(Q1,b,m,So,nL,nH,yL,yH,Cd,Cb,vd,D)
% Using the bisection method to iterate on a solution for the Manning's
% equation based on the Baptist approach for estimating n.
nM=(nL+nH)/2;
% perform calcs for n Low
    [ynL,UL,RL] = manning_bisection(Q1,b,m,So,nL,yL,yH);
    [Ck,f,nb,resnL] = baptist(nL,ynL,RL,Cd,Cb,vd,D);
% perform calcs for n Middle
    [ynM,UM,RM] = manning_bisection(Q1,b,m,So,nM,yL,yH);
    [CkM,fM,nbM,resnM] = baptist(nM,ynM,RM,Cd,Cb,vd,D);

% perform calcs for n High
    [ynH,UH,RH] = manning_bisection(Q1,b,m,So,nH,yL,yH);
    [Ck,f,nb,resnH] = baptist(nH,ynH,RH,Cd,Cb,vd,D);

while abs (resnM) > 0.1
    if (resnM * resnH) < 0
        nL = nM;
        nM=(nL+nH)/2;
% perform calcs for n Low
        [ynL,UL,RL] = manning_bisection(Q1,b,m,So,nL,yL,yH);
        [Ck,f,nb,resnL] = baptist(nL,ynL,RL,Cd,Cb,vd,D);

% perform calcs for n Middle
        [ynM,UM,RM] = manning_bisection(Q1,b,m,So,nM,yL,yH);
        [CkM,fM,nbM,resnM] = baptist(nM,ynM,RM,Cd,Cb,vd,D);

% perform calcs for n High
        [ynH,UH,RH] = manning_bisection(Q1,b,m,So,nH,yL,yH);
        [Ck,f,nb,resnH] = baptist(nH,ynH,RH,Cd,Cb,vd,D);

    else
        nH = nM;
        nM=(nL+nH)/2;
% perform calcs for n Low
        [ynL,UL,RL] = manning_bisection(Q1,b,m,So,nL,yL,yH);
        [Ck,f,nb,resnL] = baptist(nL,ynL,RL,Cd,Cb,vd,D);

% perform calcs for n Middle
        [ynM,UM,RM] = manning_bisection(Q1,b,m,So,nM,yL,yH);
        [CkM,fM,nbM,resnM] = baptist(nM,ynM,RM,Cd,Cb,vd,D);

% perform calcs for n High
        [ynH,UH,RH] = manning_bisection(Q1,b,m,So,nH,yL,yH);
        [Ck,f,nb,resnH] = baptist(nH,ynH,RH,Cd,Cb,vd,D);

    end
    fb=fM;
    nb=nbM;
    Ckb=CkM;
    yb=ynM;
end
```

Baptist normal code:

```

% Input Channel Variables
Q1=2520;
b=122;
m=2;
So=0.00125;
nL=0.01;
nH=5;
yL=0.01;
yH=100;

% Input Vegetation Variables (constant parameters set in baptist.m)
% Cb=100; % Chezy coefficient for the streambed
vd=1.5; % Vegetation density, designated as 'm' in Baptist
D=0.5; % Mean stem diameter

% Vegetation uncertainty loop
nsamples=10000
for i=1:nsamples
    Cd=normrnd(1.5,0.1);
    CdH(i)=Cd;
    Cb=normrnd(50,10);
    [ f(i),n(i),y(i),Ck(i) ] =
baptist_bisection(Q1,b,m,So,nL,nH,yL,yH,Cd,Cb,vd,D);
end
    mean(n)
    std(n)
    mean(y)
    std(y)

```

Baptist single code:

```
% Baptist with a Uniform input distribution
% Input Channel Variables
Q1=.008;
b=1;
m=0;
So=0.003;
nL=0.001;
nH=5;
yL=0.001;
yH=100;

% Input Vegetation Variables (constant parameters set in baptist.m)
% Cb=100; % Chezy coefficient for the streambed
vd=100; % Vegetation density, designated as 'm' in Baptist
D=0.025; % Mean stem diameter
Cd=1.5
Cb=100

[ f,n,y,Ck ] = baptist_bisection(Q1,b,m,So,nL,nH,yL,yH,Cd,Cb,vd,D);
```

Manning bisection code:

```
function [yn,U,R] = manning_bisection(Q1,b,m,So,n,yL,yH)
%UNTITLED6 Summary of this function goes here
% Detailed explanation goes here

yM=(yL+yH)/2;
[resL,U,R]=manning_trap(Q1,b,m,So,n,yL);
[resM,Um,Rm]=manning_trap(Q1,b,m,So,n,yM);
[resH,U,R]=manning_trap(Q1,b,m,So,n,yH);

while abs (resM) > 0.01
    if (resM * resH) < 0
        yL = yM;
        yM=(yL+yH)/2;
        [resL,U,R]=manning_trap(Q1,b,m,So,n,yL);
        [resM,Um,Rm]=manning_trap(Q1,b,m,So,n,yM);
        [resH,U,R]=manning_trap(Q1,b,m,So,n,yH);
    else
        yH = yM;
        yM=(yL+yH)/2;
        [resL,U,R]=manning_trap(Q1,b,m,So,n,yL);
        [resM,Um,Rm]=manning_trap(Q1,b,m,So,n,yM);
        [resH,U,R]=manning_trap(Q1,b,m,So,n,yH);
    end
end
yn=yM;
U=Um;
R=Rm;
end
```


Normal Distribution code:

```
% Input Channel Variables
Q1=2520,
b=122,
m=2,
So=0.00125,
nL=0.01,
nH=5,
yL=0.01,
yH=100,

% Input Vegetation Variables (constant parameters set in baptist.m)
% Cb=100, % Chezy coefficient for the streambed
vd=10, % Vegetation density, designated as 'm' in Baptist
D=0.5, % Mean stem diameter

% Vegetation uncertainty loop
nsamples=10000
for i=1:nsamples
    Cd=normrnd(1.5,0.1),
    CdH(i)=Cd,
    Cb=normrnd(50,10),
    [ f(i),n(i),y(i),Ck(i) ] =
baptist_bisection(Q1,b,m,So,nL,nH,yL,yH,Cd,Cb,vd,D),
end
    mean(n)
    std(n)
    mean(y)
    std(y)
```

Jarvela (2004) Approach

Uniform Distribution code:

```
% Jarvela with a Uniform distribution for input parameters
% Input Channel Variables
Q1=2520,
b=122,
m=2,
So=0.00125,
nL=0.01,
nH=2,
yL=0.1,
yH=100,

% Input Vegetation Variables (additional data specified in jarvela.m)
LAI=1,

% Vegetation uncertainty loop
nsamples=1000
for i=1:nsamples
    X=-0.6+rand(1)*0.15,
    Xh(i)=X,
    Cd=0.4+rand(1)*0.15,
    Cdh(i)=Cd,
    [f(i),n(i),y(i)] =
jarvela_bisection(Q1,b,m,So,nL,nH,yL,yH,X,LAI,Cd),
end
    mean(n)
    std(n)
    mean(y)
    std(y)
```

Jarvela bisection code:

```
function [fj,nj,resn] = jarvela(n1,U,y,R,X,LAI,Cd)
%Vegetation input data
Uz=0.1;
H=5;
g=9.81;

% Jarvela Calculation
fj=4*Cd*LAI*((U/Uz)^X)*(y/H);
nj=(R^0.1667)*((fj/(8*g))^0.5);
resn=((nj-n1)/n1)*100;
end
```

Normal Distribution code:

```
% Input Channel Variables
Q1=2520,
b=122,
m=2,
So=0.00125,
nL=0.01,
nH=2,
yL=0.1,
yH=100,

% Input Vegetation Variables (additional data specified in jarvela.m)
LAI=1.0,

% Vegetation uncertainty loop
nsamples=100
for i=1:nsamples
    X=normrnd(-0.5,0.03),
    Xh(i)=X,
    Cd=normrnd(0.5,0.03),
    Cdh(i)=Cd,
    [f(i),n(i),y(i)] =
jarvela_bisection(Q1,b,m,So,nL,nH,yL,yH,X,LAI,Cd),
end
    mean(n)
    std(n)
    mean(y)
    std(y)
```

Manning bisection code:

```
function [yn,U,R] = manning_bisection(Q1,b,m,So,n,yL,yH)
% Determines an iterative solution for the Manning's equation.

yM=(yL+yH)/2;
[resL,U,R]=manning_trap(Q1,b,m,So,n,yL);
[resM,Um,Rm]=manning_trap(Q1,b,m,So,n,yM);
[resH,U,R]=manning_trap(Q1,b,m,So,n,yH);

while abs (resM) > 0.01
    if (resM * resH) < 0
        yL = yM;
        yM=(yL+yH)/2;
        [resL,U,R]=manning_trap(Q1,b,m,So,n,yL);
        [resM,Um,Rm]=manning_trap(Q1,b,m,So,n,yM);
        [resH,U,R]=manning_trap(Q1,b,m,So,n,yH);
    else
        yH = yM;
        yM=(yL+yH)/2;
        [resL,U,R]=manning_trap(Q1,b,m,So,n,yL);
        [resM,Um,Rm]=manning_trap(Q1,b,m,So,n,yM);
        [resH,U,R]=manning_trap(Q1,b,m,So,n,yH);
    end
end
yn=yM;
U=Um;
R=Rm;
end
```

Jarvela.m code:

```
function [fj,nj,resn] = jarvela(n1,U,y,R,X,LAI,Cd)
%Vegetation input data
Uz=0.1;
H=5;
g=9.81;

% Jarvela Calculation
fj=4*Cd*LAI*((U/Uz)^X)*(y/H);
nj=(R^0.1667)*((fj/(8*g))^0.5);
resn=((nj-n1)/n1)*100;
end
```

Turbulence Characteristics Code:

```
% Specify the input file name (currently based on Excel)
filename = 'Flume_Data.xlsx';
sheet = 1;
uRange = 'A2:A3001';
vRange = 'B2:B3001';
wRange = 'C2:C3001';
    u = xlsread(filename, sheet, uRange);
    v = xlsread(filename, sheet, vRange);
    w = xlsread(filename, sheet, wRange);
ubar=mean(u);           % Find the mean values
vbar=mean(v);
wbar=mean(w);
uprime=u(:)-ubar;      % Calculate the fluctuating time series
vprime=v(:)-vbar;
wprime=w(:)-wbar;
TIx=std(uprime);       % Calculate the turbulence intensities
TIy=std(vprime);
TIz=std(wprime);
TKE=(mean(uprime.^2)+mean(vprime.^2)+mean(wprime.^2))/2; % Calc TKE
covuv=cov(u,v);       % Calc covariance coefficients
covuw=cov(u,w);
covvw=cov(v,w);
tauuv=-9.9900e-04*covuv(1,2); % Calc the RSS values
tauuw=-9.9900e-04*covuw(1,2);
tauvw=-9.9900e-04*covvw(1,2);
N=length(u);          % Prepare to calculate autocorrelations
H=round(N/2);
up=zeros(1,N);
R=zeros(1,H);
for d=1:H % d for delta, within this, calculate autocorrelations for
series of deltas
    g=0;
    for k=1: N-d
        up(k)=u(k+d);
    end;
    f=N-d+1;
    for i=f: N
        g=g+1;
        up(i)=u(g);
    end
    covup=cov(u,up);
    corup=corrcoef(u,up);
    R(d)=corup(1,2); % Autocorrelation coefficient
end
summit=cumtrapz(R); % Compute the cumulative integral of R
ms=max(summit); % Find the peak in the cumulative integration,
indicates when R<0
spot=find(summit>ms-0.01,1); % Find array location for peak value
Rtruc=R; % Copy R in order to truncate
Rtruc(spot:g)=[]; % Truncate the R function after R<0
Tx=trapz(Rtruc)*0.04; % Integrate the function, multiply by delta t,
gives Integral Time Scale
Lx=Tx*ubar; % Estimate integral length scale from Taylor's hypothesis
```

Appendix C- Roughness Calculation Spreadsheet





Department of Civil Engineering, University of New Mexico-USA

Spreadsheet name: Roughness Calculation Aid

By: Abdou Harissou¹, Dr. Stone² & Dr. Chen³
 1 & 2 at the University of New Mexico-USA
 3 at Desert Research Institute, Las Vegas, Nevada-USA

Objective: Help in computing vegetation hydraulic roughness in open channel flows with emergent canopies
 This spreadsheet is intend to provide a rapid vegetation roughness assessment for the users.

Input/Outputs infos: Cell Color Attributes

-  Input Data
-  Output/Results
-  Output of Interest
-  Error Estimate

Notation:

Q, Flow discharge with the stream
 b, Channel bed width
 S_o, Channel bed slope
 S_f, Friction slope
 s_v, Vegetation spacing
 d_v, Vegetation stem diameter
 H, Flow depth
 h_p, Vegetation height
 y_n, Flow depth
 A, Momentum absorbing area or projected area
 P, Wetted perimeter of the channel
 R, Hydraulic radius
 U_o, Approched velocity
 U_v, Velocity within the vegetation
 f, Darcy-Weisbach friction factor
 τ, Boundary shear stress
 n, Manning's n
 Q_{calc}, Flow discharge computed
 Error, Estimation of error between Q_{measured} and Q_{computed}
 m, Vegetation density
 D, Vegetation diameter
 C_D, Drag coefficient
 C_B, Chezy coefficient of the stream bed

Constants:

g, Acceleration due to gravity
 a, Velocity Coefficient
 z₁, Datum
 K, Units
 ρ, Fluid mass density
 ξE, Vegetation index
 MEI, Vegetation rigidity

Approach 1: For non-submerged or Emergent and Rigid Vegetation within unifer flow
 Based on: Thomson and Roberson (1976) and Darby (1999)

Known Parameters

Q_v= 0.1
 S_v= 0.002
 Guess H 0.10
 A 0.1
 U_{z=0} 1.000

Vegetation info

s_v= 0.08
 d_v= 0.025

Relative Spacing

S_v/d_v= 10

Normal Depth Calculations

U_{wake} 0.563
 f 0.0358
 n 0.015
 H -85.5

Known Parameters

U_{z=0} 1
 S_v= 0.002
 R 0.50

Vegetation info

s_v= 0.08
 d_v= 0.025

Relative Spacing

S_v/d_v= 20

Normal Depth Calculations

U_{wake} 0.000

Constants (SI units)

g= 9.81 m/s²
 ν= 0.000001 m²/s

Uwake: In-canopy velocity calcs options for rigid stems

| 4<S _v /d _v <20 | 20<S _v /d _v <100 | S _v /d _v >100 |
|--------------------------------------|--|-------------------------------------|
| 0.663 | 0.842 | 1.000 |

Re= 100000

| Relative Spacing | 4<S _v /d _v <20 | 20<S _v /d _v <100 | S _v /d _v >100 | U _{rt} |
|------------------|--------------------------------------|--|-------------------------------------|-----------------|
| 4 | 0.583 | 0.782 | 1.000 | 0.583 |
| 6 | 0.617 | 0.808 | 1.000 | 0.617 |
| 8 | 0.642 | 0.827 | 1.000 | 0.642 |
| 10 | 0.663 | 0.842 | 1.000 | 0.663 |
| 12 | 0.680 | 0.854 | 1.000 | 0.680 |
| 14 | 0.695 | 0.865 | 1.000 | 0.695 |
| 16 | 0.708 | 0.874 | 1.000 | 0.708 |
| 18 | 0.719 | 0.882 | 1.000 | 0.719 |
| 20 | 0.730 | 0.890 | 1.000 | 0.890 |
| 25 | 0.753 | 0.906 | 1.000 | 0.906 |
| 30 | 0.773 | 0.919 | 1.000 | 0.919 |
| 40 | 0.805 | 0.940 | 1.000 | 0.940 |
| 50 | 0.830 | 0.957 | 1.000 | 0.957 |
| 60 | 0.851 | 0.971 | 1.000 | 0.971 |
| 70 | 0.870 | 0.983 | 1.000 | 0.983 |
| 80 | 0.886 | 0.994 | 1.000 | 0.994 |
| 90 | 0.901 | 1.003 | 1.000 | 1.003 |
| 100 | 0.915 | 1.012 | 1.000 | 1.012 |

Constants (SI units)

g= 9.81 m/s²
 ν= 0.000001 m²/s

Uwake: In-canopy velocity calcs options for rigid stems

| 4<S _v /d _v <20 | 20<S _v /d _v <100 | S _v /d _v >100 |
|--------------------------------------|--|-------------------------------------|
| 0.730 | 0.890 | 1.000 |

Re= 500000

| Relative Spacing | 4<S _v /d _v <20 | 20<S _v /d _v <100 | S _v /d _v >100 | U _{rt} |
|------------------|--------------------------------------|--|-------------------------------------|-----------------|
| 4 | 0.583 | 0.782 | 1.000 | 0.583 |
| 6 | 0.617 | 0.808 | 1.000 | 0.617 |
| 8 | 0.642 | 0.827 | 1.000 | 0.642 |
| 10 | 0.663 | 0.842 | 1.000 | 0.663 |
| 12 | 0.680 | 0.854 | 1.000 | 0.680 |
| 14 | 0.695 | 0.865 | 1.000 | 0.695 |
| 16 | 0.708 | 0.874 | 1.000 | 0.708 |
| 18 | 0.719 | 0.882 | 1.000 | 0.719 |
| 20 | 0.730 | 0.890 | 1.000 | 0.890 |
| 25 | 0.753 | 0.906 | 1.000 | 0.906 |
| 30 | 0.773 | 0.919 | 1.000 | 0.919 |
| 40 | 0.805 | 0.940 | 1.000 | 0.940 |
| 50 | 0.830 | 0.957 | 1.000 | 0.957 |
| 60 | 0.851 | 0.971 | 1.000 | 0.971 |
| 70 | 0.870 | 0.983 | 1.000 | 0.983 |
| 80 | 0.886 | 0.994 | 1.000 | 0.994 |
| 90 | 0.901 | 1.003 | 1.000 | 1.003 |
| 100 | 0.915 | 1.012 | 1.000 | 1.012 |

Approach 2: For Emergent, Flexible Vegetations ,Kouwen and Fathi (2000)

| Known Parameters | | Constants (SI units) | | Definition of Input Parameter | |
|------------------|-------------|----------------------|-------|-------------------------------|--------------------------------|
| Q= | 0.098 | g= | 9.81 | KsIE | Vegetation index |
| b= | 0.942 | a= | 1 | H | Flow deth |
| So= | 0.003 | ±1= | 0 | hp | Vegetation height |
| Sf= | 0.003 | K= | 1 | R | Hydraulic radius replaced by H |
| hp= | 1.129961657 | p= | 1.000 | | |

Percent error = $\frac{\text{Measured-Cal}}{\text{Calc}} \times 100$

| Species | KsiE |
|---------------|------|
| Cedar | 2.07 |
| White pine | 2.99 |
| Spruce | 3.36 |
| Austrian pine | 4.54 |

Calculation of Manning's n by guessing flow depth

| | | |
|------------------|-------------|------------------------|
| R = H guess | 0.564980828 | |
| Choose KsiE | 20 | KsiE for Austrian pine |
| A = | 0.53221194 | |
| U ₀ = | 0.184137169 | |
| f = | 1.82086723 | |
| n = | 0.2006198 | |
| Q Calc | 0.099302581 | |
| error | | |

| KsiE | n | y or H | hp |
|------|-------------|-------------|-----|
| 1 | 0.0441306 | 0.22595 | 0.1 |
| 2 | 0.0893343 | 0.34497 | 0.2 |
| 3 | 0.1210748 | 0.414001 | 0.3 |
| 4 | 0.1425634 | 0.4566396 | 0.4 |
| 5 | 0.157371 | 0.48453 | 0.5 |
| 6 | 0.167882 | 0.50370 | 0.6 |
| 7 | 0.175571 | 0.5174172 | 0.7 |
| 8 | 0.1813505 | 0.52757 | 0.8 |
| 9 | 0.1857985 | 0.53530 | 0.9 |
| 10 | 0.1892928 | 0.541315 | 1 |
| 11 | 0.1920865 | 0.54609255 | 1.1 |
| 12 | 0.1943548 | 0.54995181 | 1.2 |
| 13 | 0.1962212 | 0.55311412 | 1.3 |
| 14 | 0.1977749 | 0.55574 | 1.4 |
| 15 | 0.199082 | 0.5579379 | 1.5 |
| 16 | 0.2001907 | 0.55980 | 1.6 |
| 17 | 0.2011396 | 0.561392 | 1.7 |
| 18 | 0.201957522 | 0.562760393 | 1.8 |
| 19 | 0.202667054 | 0.563945986 | 1.9 |
| 20 | 0.20328622 | 0.564979236 | 2 |

Y vs. n

KsiE vs. n

Approach 3: For Emergent, Flexible vegetation, (Jarvelar, 2004)

| Known Parameters | | | Constants (SI units) | | |
|------------------|-------|-----|----------------------|--|--|
| Q= | 0.015 | g= | 9.81 | | |
| b= | 0.942 | a= | 1 | | |
| So= | 0.003 | z1= | 0 | | |
| Sf= | 0.003 | K= | 1 | | |
| H | 0.419 | p= | 1000 | | |
| Cdr= | 0.7 | | | | |
| r _f = | -0.5 | | | | |
| U _r = | 0.1 | | | | |

R_f for Willow

H < h_p for emergent vegetation

Definition of Input Parameter

- Cdr: Species-specific drag coef
- LAI: Leaf area index
- U_r: Reference velocity
- r_f: Species-specific exponent
- U: Velocity in x direction
- V: Velocity in y direction
- h: Flow depth
- R: Hydraulic radius (replaced by H)
- f: Darcy-Weisbach friction coefficient
- n: Manning's n
- H: Vegetation height

Calculation of Manning's n by guessing flow depth

| | |
|------------------|---------|
| h Guess | 0.209 m |
| Choose LAI | 4.270 |
| A | 0.197 |
| R | 0.145 |
| U ₀ = | 0.076 |
| h/H | 0.500 |
| f | 5.214 |
| n | 0.199 |
| Q Calc | 0.015 |
| error | 0.000 |

Table of Species and their respective index vs

| Species | KsiE | Cdr | Ur (m/) |
|---------------|------|------|---------|
| Cedar | 2.07 | 0.56 | 0.1 |
| White pine | 2.99 | 0.69 | 0.1 |
| Spruce | 3.36 | 0.57 | 0.1 |
| Austrian pine | 4.54 | 0.45 | 0.1 |
| Willow | - | 0.43 | 0.1 |

Table of Cdr = 0.4

| LAI | n | f |
|------|------------|-------------|
| 0.10 | 0.02566979 | 0.135703254 |
| 0.25 | 0.03967049 | 0.29578904 |
| 0.75 | 0.06682763 | 0.751053178 |
| 1.02 | 0.07732246 | 0.974294608 |
| 1.34 | 0.08800468 | 1.22710451 |
| 1.67 | 0.09768695 | 1.47789343 |
| 1.99 | 0.10615128 | 1.713570645 |
| 2.32 | 0.1141573 | 1.950906326 |
| 2.64 | 0.12136467 | 2.174716147 |
| 2.97 | 0.1283291 | 2.401566883 |
| 3.29 | 0.13470217 | 2.617655038 |
| 3.62 | 0.14094023 | 2.836934822 |

Table of Cdr = 0.5

| LAI | n | f |
|------|------------|------------|
| 0.10 | 0.02854109 | 0.1640817 |
| 0.25 | 0.04410495 | 0.35750371 |
| 0.75 | 0.07429015 | 0.907197 |
| 1.02 | 0.08595398 | 1.176609 |
| 1.34 | 0.09782547 | 1.481627 |
| 1.67 | 0.10858518 | 1.784132 |
| 1.99 | 0.11799106 | 2.068355 |
| 2.32 | 0.12688734 | 2.353805 |
| 2.64 | 0.13489593 | 2.624351 |
| 2.97 | 0.14263437 | 2.89780263 |
| 3.29 | 0.14971554 | 3.15824784 |
| 3.62 | 0.15664656 | 3.42250919 |

Table of Cdr = 0.6

| LAI | n | f |
|------|-------------|------------|
| 0.10 | 0.031123621 | 0.19160856 |
| 0.25 | 0.04809304 | 0.4173376 |
| 0.75 | 0.081000522 | 1.05846995 |
| 1.02 | 0.093715137 | 1.37256296 |
| 1.34 | 0.106655575 | 1.72808824 |
| 1.67 | 0.118383652 | 2.08061445 |
| 1.99 | 0.128635718 | 2.41177863 |
| 2.32 | 0.138332068 | 2.74432405 |
| 2.64 | 0.147060674 | 3.05946582 |
| 2.97 | 0.155494636 | 3.37795399 |
| 3.29 | 0.16321211 | 3.68126118 |
| 3.62 | 0.17076578 | 3.98898212 |

Table of Cdr = 0.7

| LAI | n |
|------|---------|
| 0.10 | 0.03348 |
| 0.25 | 0.05174 |
| 0.75 | 0.08714 |
| 1.02 | 0.10081 |
| 1.34 | 0.11473 |
| 1.67 | 0.12735 |
| 1.99 | 0.13837 |
| 2.32 | 0.14880 |
| 2.64 | 0.15819 |
| 2.97 | 0.16726 |
| 3.29 | 0.17556 |
| 3.62 | 0.18368 |

Instructions #1 T&R 76 - E R #2 K&F 00 E F #3 Jarvela 04 E F #4 Baptist 07 E&S R #5 K&L 80 S F Nassam Test

Approach 4: For Emergent and Rigid Vegetation within uniform flow stream
 Based on: M.J. Baptist (2007)
 Note: Chezy Coefficient of the stream bed in considered during this computing process

Known Parameters

Q= 0.098
 b= 0.942
 S₀= 0.003

Constants (SI units)

g= 9.81
 a= 1.00
 z_v= 0.00
 K= 1.00

Definitions of Input Parameters

C_b Chezy's coefficient of the flume bed with no vegetation
 C_r Chezy's coefficient
 DEF Sediment diameter that 84% is finer (for C_b estimation)
 C_D Drag Coefficient
 D Stem diameter
 H Flow depth
 R Hydraulic radius (replaced by U)
 h_p Vegetation height

Vegetation infos

m= 30
 D= 0.025
 C_D= 0.8
 C_e= 62
 h_p= 2.26739
 kappa= 0.41

Output Parameters

f Darcy-weisbach friction coef
 n Manning's n

Normal Depth Calculations

R=H_{gue} 1.13
 A= 1.07
 P= 3.21
 R= 0.33
 C_r= 5.37
 U= 0.17
 Cr 1.49
 n 0.80570
 Q Calc 0.0789
 error 24.164

| Cd = 0.4 | | | | | |
|----------|-------|-------|---------|----------|--|
| m | D | mD | n | f | |
| 5 | 0.025 | 0.125 | 0.05995 | 22.36219 | |
| 10 | 0.025 | 0.25 | 0.09530 | 13.68111 | |
| 15 | 0.025 | 0.375 | 0.1318 | 9.72118 | |
| 20 | 0.025 | 0.5 | 0.171 | 7.392977 | |
| 25 | 0.025 | 0.625 | 0.21467 | 5.828386 | |
| 30 | 0.025 | 0.75 | 0.2647 | 4.68405 | |
| 35 | 0.025 | 0.875 | 0.3242 | 3.79403 | |
| 40 | 0.025 | 1 | 0.3982 | 3.065357 | |
| 45 | 0.025 | 1.125 | 0.4971 | 2.436661 | |
| 50 | 0.025 | 1.25 | 0.64896 | 1.851096 | |
| 55 | 0.025 | 1.375 | 1.0598 | 1.118911 | |
| 60 | 0.025 | 1.5 | | | |
| 65 | 0.025 | 1.625 | | | |
| 70 | 0.025 | 1.75 | | | |
| 75 | 0.025 | 1.875 | | | |
| 80 | 0.025 | 2 | | | |
| 85 | 0.025 | 2.125 | | | |
| 90 | 0.025 | 2.25 | | | |
| 95 | 0.025 | 2.375 | | | |
| 100 | 0.025 | 2.5 | | | |

| Cd = 0.6 | | | | | |
|----------|-------|-------|---------|------|--|
| m | D | mD | n | | |
| 5 | 0.025 | 0.125 | 0.07760 | 17.1 | |
| 10 | 0.025 | 0.25 | 0.13178 | 9.7 | |
| 15 | 0.025 | 0.375 | 0.1922 | 6.5 | |
| 20 | 0.025 | 0.5 | 0.2647 | 4.6 | |
| 25 | 0.025 | 0.625 | 0.35888 | 3.4 | |
| 30 | 0.025 | 0.75 | 0.4971 | 2.4 | |
| 35 | 0.025 | 0.875 | 0.7751 | 1.5 | |
| 40 | 0.025 | 1 | | | |
| 45 | 0.025 | 1.125 | | | |
| 50 | 0.025 | 1.25 | | | |
| 55 | 0.025 | 1.375 | | | |
| 60 | 0.025 | 1.5 | | | |
| 65 | 0.025 | 1.625 | | | |
| 70 | 0.025 | 1.75 | | | |
| 75 | 0.025 | 1.875 | | | |
| 80 | 0.025 | 2 | | | |
| 85 | 0.025 | 2.125 | | | |
| 90 | 0.025 | 2.25 | | | |
| 95 | 0.025 | 2.375 | | | |
| 100 | 0.025 | 2.5 | | | |

mD vs. f

mD vs. n

Instructions #1 T&R 76 - E_R #2 K&F 00 - E_F #3 Jarvela 04 - E_F #4 Baptist 07 E&S_R #5 K&L 80 - S_F Nassam Test

Approach 5: For Emergent and Rigid Vegetation within uniform flow stream, Kouwen and Li (1980)
 Note: This method takes into account the total drag force within the system

Known Parameters

| | |
|---------|-------|
| Q= | 500 |
| b= | 0.942 |
| S_c = | 0.003 |
| S= | 0.003 |

Vegetation

| | |
|--------------|-----------|
| m= | 86 |
| D= | 0.025 |
| C_D = | 1 |
| A, projected | 0.058 |
| hp= | 299.73271 |

Normal Depth Calculations

| | |
|------------|-----------|
| R=H, guess | 149.86635 |
| Area | 141.17411 |
| P | 300.67471 |
| U_o | 3.541726 |
| R | 0.4695 |
| k | 0.0 |
| f | 0.0012895 |
| n | 0.00934 |
| Q, Calc | 499.9999 |
| error | 0.009 |

Quick check
 U_{calc} = 3.5417

UR= 530.7855626

Constants (SI units)

| | |
|----------|------|
| g= | 9.81 |
| a= | 1.00 |
| z_i = | 0.00 |
| K= | 1.00 |
| ρ = | 1000 |
| MEI = | 1 |

as (suggested by Li) = 12.2
 a_s = 12.20
 a_s = 0.0

Definitions of Input Parameters

| | |
|--------|-------------------------------|
| MEI | Vegetation rigidity |
| hp | undeflected vegetation height |
| Sf | friction slope |
| ρ | flow density |
| H | Flow depth |
| a_s | Shape factor |

Output Parameters

| | |
|---|------------------------------|
| k | deflected vegetation height |
| f | Darcy-weisbach friction coef |
| n | Manning's n |

| hp | n | y | f |
|-----|-------------|-------------|-------------|
| 0.1 | 0.0886594 | 0.07297024 | 1.47625032 |
| 0.2 | 0.11841742 | 0.12299 | 2.21290 |
| 0.3 | 0.13975351 | 0.17023 | 2.76569 |
| 0.4 | 0.15652845 | 0.21627159 | 3.20340913 |
| 0.5 | 0.17031873 | 0.26169196 | 3.55921072 |
| 0.6 | 0.18196594 | 0.30677454 | 3.85300 |
| 0.7 | 0.19199329 | 0.35167016 | 4.09844636 |
| 0.8 | 0.20074805 | 0.3964729 | 4.3051719 |
| 0.9 | 0.208478 | 0.44124114 | 4.48044153 |
| 1 | 0.21536221 | 0.48601853 | 4.62963842 |
| 1.1 | 0.22154137 | 0.53083001 | 4.75719 |
| 1.2 | 0.22712337 | 0.57569512 | 4.86651936 |
| 1.3 | 0.23219412 | 0.62062775 | 4.96041 |
| 1.4 | 0.236829073 | 0.665637861 | 5.041128 |
| 1.5 | 0.24106718 | 0.710732635 | 5.11053561 |
| 1.6 | 0.244973663 | 0.755917264 | 5.170188421 |
| 1.7 | 0.248582088 | 0.80119533 | 5.221386671 |
| 1.8 | 0.251925906 | 0.846569475 | 5.265227243 |
| 1.9 | 0.255033621 | 0.892041382 | 5.302640716 |
| 2 | 0.257929696 | 0.937612121 | 5.334420923 |

hp vs. n

Instructions #1 T&R 76 - E_R #2 K&F 00 E_F #3 Jarvela 04 E_F #4 Baptist 07 E&S_R #5 K&L 80 S_F Nassam Test

Appendix D - Conceptual model development

Nepf *et al.* (2007) suggested that for submerged canopies of sufficient density, the dominant characteristic of the flow is the generation of a shear-layer at the top of the canopy. The shear-layer generates coherent vortices due to Kelvin-Helmholtz (KH) phenomenon. These vortices control the exchange of the mass and momentum.

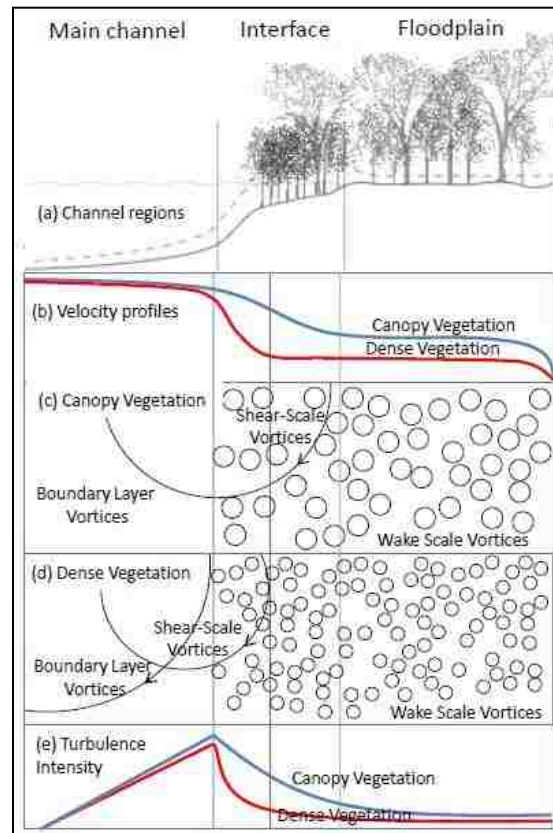


Figure 20: Schematic of the conceptual model

Figure 1 illustrates the physics taking place within the channel in general and more specifically at the stream flow and floodplain interface. In region (a) of the scheme, as the flow accelerates down the channel momentum is created due to gravity. It is absorbed/ dissipated as energy throughout the flow due to the making and breakings of eddies, Thom (1971), or carried into the floodplains. The penetration length (δ_e)

represents the distance the KH vortices travel into the floodplain and can be evaluated using Nepf (2008) equation (7) or by using profiles of Reynolds' stress as suggested in Nepf et al. (2007).

In region (b), longitudinal mixing is observed within the channel. These processes are described in detail in Shucksmith *et al.* (2010). The mixing coefficients in open channel flow are commonly scaled against the product of flow depth and shear velocity, hu^* . Longitudinal mixing coefficients may be obtained from the change in variance of tracer profiles with distance over time using the standard method moments use. This method has been used intensively in Rutherford (1994).

There are a few different ways of evaluating shear velocities that contribute to the longitudinal mixing. Such as 1) determining the best fit value of u^* when fitting the velocity profiles to the measured vertical profiles of primary velocities, 2) by the method proposed by Babaeyan *et al.* (2002), which suggested the interpolation of 3 lines of measured distribution of Reynolds stresses, or by 3) the theoretical method which uses the equation

$$u^* = \sqrt{gRS_o} \quad (5)$$

where R is the hydraulic radius, S_o is the channel bottom or bed slope.

In region (c) and (d), as momentum travels through the vegetative stems, the exchange of mass and the velocity differentials provokes eddies and shear layer formation. The density of the riparian canopy is a key factor in floodplain momentum

transfer. A dense canopy will act like a wall and prevent any substantial penetration, whereas a sparse canopy readily allows a flood wave to enter and attenuate its flow.

The production of turbulence within stem wakes surpasses the production through bed shear even for sparse vegetative canopies Nepf *et al.* (1997). However, turbulence intensity depends greatly on canopy density as shown in region (e), on the assumption that canopy is homogeneous, the turbulent kinetic energy budget is just the balance between the viscous dissipation and wake production around each stems. The equation used in calculating the turbulence intensity is

$$\frac{\sqrt{k}}{U} = \alpha_1 [\overline{C_D} ad]^{1/3} \quad (6)$$

where α_1 is a scale coefficient, k is the turbulent kinetic energy per unit mass, $\frac{\sqrt{k}}{U}$ is the turbulence intensity, ad is the canopy density, C_D is the bulk drag coefficient.

Turbulence intensity is one the important constituency driving momentum in out floodplain. It has to be model in order to characterized resistance of flow through vegetative elements. A 3-D model using a simplified Navier-Stokes equation to get a 1-D model can be used. Various simplifications are done to account for horizontal flow conditions, Baptist (2007). Some modifications suggested in Baptist (2007) are needed to be made prior to running the model. These modifications includes decrease of available cross-section for momentum exchange in vertical direction, the turbulence kinetic energy and turbulent dissipation, the horizontal drag force, turbulence produced and dissipated

by vegetative elements. This 1-D model assumes the flow is uniform in horizontal direction. The equation used in computing the momentum is

$$\rho \frac{\partial u}{\partial t} + \frac{\partial p}{\partial x} = \frac{\partial}{\partial z} \frac{\partial}{\partial z} \left((1 - A)(\nu + \nu_T) \frac{\partial u}{\partial z} \right) - \frac{F}{1 - A} \quad (7)$$

where F is the drag force of the vegetative elements per unit volume (Nm^{-3}), A is the stems frontal area, solidity, ν is the kinematic viscosity of water (m^2/s), ν_t is the viscosity of the eddies in wakes (m^2/s), ρ is the density of water (kg/m^3).

Momentum and Mass within the system

In Nepf (1997), a mixing of momentum and mass was observed during an experiment conducted with dowel rods with constant distribution of mass over a given flow depth. It was also found that in cases where vortices generated by shear layer are present, mixing takes place rapidly, otherwise when wake zones exists, mixing takes longer. However, a decrease in longitudinal mixing coefficient was noticed relative to non-vegetated flow. Shucksmith et al. (2010) suggested that distributing emergent vegetation in an even fashion over the entire width of natural channel has better chances of reducing spatial variation of velocity over the channel width, depth and Reynolds stresses.

In the case of emergent vegetation within a stream, as water flows through the channel, the momentum is created in the stream by the gravity, and the flux is carried throughout the stream and into the floodplains. At the interface of flow and floodplains,

the momentum is either absorbed by the vegetative canopies (when dense) or travels/penetrates into the highland in case low floodplains. This momentum penetration (δ_e) was described by Nepf *et al.* (2008) and its equation is

$$\frac{\delta_e}{h} = \frac{0.26 \pm 0.06}{C_D a h} \quad (8)$$

Momentum flux across the channel is a crucial component in investigating vegetation roughness within streams and rivers. In emergent vegetated streams, the majority of flow momentum is absorbed by the vegetation elements as drag rather than the bed resistance, Shucksmith *et al.* (2010). The vertical velocity profiles in artificial emergent vegetation have a strong correlation with the distribution of mass within the vegetation Lightbody *et al.* (2006).

The viscous and drag force F_r per fluid mass due to vegetation roughness may be described as

$$F_r = \left[\frac{\text{force}}{\text{mass}} \right] = (f_d + f_v) = \frac{1}{2} \overline{C_D} m U^2 \quad (9)$$

$$f_d = -\frac{1}{\rho V_f} \int \int_{S_{int}} \bar{p} n_x dS_{int} \quad (10-a)$$

$$f_v = -\frac{1}{V_f} \int \int_{S_{int}} V \frac{\partial \bar{u}}{\partial n_{int}} dS_{int} \quad (10-b)$$

where f_d is the drag force due to stream bed and f_v is the drag force due to the vegetation roughness, U is the equivalent uniform velocity, C_D is the bulk drag coefficient, m the vegetation density (per meter) is the projected stem area per unit volume, the integral (10-a) and (10-b) are taken over the surfaces of the elements intersecting the average volume, with S_{int} the sum of all such interval areas, n_{int} is the unit normal vector on a given direction (n_x , n_y , or n_z). If the stems are modeled as cylinders, then

$$m = nd = \frac{dh}{\Delta S^2 h} = \frac{d}{\Delta S^2} \quad (11)$$

where n is the number of stems per unit area, that is, plants per square meter, ΔS is the mean spacing between stems, d is the stem diameter, and h is the flow depth.

Inside the vegetative canopy water is forced to flow around each plant (stem) in a way that the velocity field is spatially and temporally heterogeneous at the stem scale, and a double averaging scheme accounts for this heterogeneity. Raupach et al. (1982) described this occurrence and gave more thorough explanation on the double averaging scheme. It is applied on rigid canopy that is homogeneous and the momentum equation becomes an adapted form of Navier-Stokes equation,

$$\frac{D\langle\bar{u}\rangle}{Dt} = g_x - \frac{1}{\rho n} \frac{\partial n\langle\bar{p}\rangle}{\partial x} - \frac{1}{n} \frac{\partial}{\partial z} n\langle\bar{u}'w'\rangle - \frac{1}{n} \frac{\partial}{\partial z} n\langle\bar{u}''w''\rangle + \frac{1}{n} \frac{\partial}{\partial z} n\nu \frac{\partial\langle\bar{u}\rangle}{\partial z} + f_d + f_v \quad (12)$$

where ν is the molecular viscosity, g_x is the component of gravitational force parallel to the bed, the term (a) represents the spatial-average of the familiar Reynolds' stress, the term (b) is the dispersive stress, arising from spatial correlations in the time-averaged field, and term (c) represents the viscous stress associated with the spatial variation in velocity at the top of the canopy.

Drag due to non-submerged canopy

Although Manning's n is not the best way use of in evaluating flow resistance because of its variability with velocity and flow depth Freeman (2000), it is however, one of the extensively used equations when characterizing drag or resistance to flow by a roughness coefficient. The roughness coefficient is obtained through Manning's general equation,

$$n = \frac{K}{V} R^{2/3} S^{1/2} \quad (13)$$

where n is the Manning's resistance coefficient, K is the unit correction factor of 1.0 For SI units, and 1.49 for non-SI units, V is the mean flow velocity, R is the hydraulic radius, and S is the energy grade slope.

Other forms of evaluating flow resistance to roughness are the Darcy-Weisbach friction factor f , Chezy coefficient C and, the ratio between shear velocities to mean velocity. These equations can easily be converted to Manning's n by equating them as the following,

$$\frac{V_*}{V} = \left(\frac{\tau_o}{\rho V^2} \right)^{1/2} = \sqrt{\frac{f}{8}} = \frac{n}{K} \sqrt{\frac{g}{R^{1/3}}} = \frac{\sqrt{g}}{C} \quad (14)$$

where V_* is the shear velocity, g is the gravitational force, τ_o is the shear stress and ρ the fluid density.

Though countless of researchers have evaluated roughness coefficient solely through the effect of stream bed and resistance due to vegetative elements. Cowan (1956) method for additive resistance proposed Manning's resistance coefficient for vegetation to take into account roughness for various surface and vegetation irregularities in order to obtain better representation of channels roughness coefficients. The method is described by the equation

$$n = (n_o + n_1 + n_2 + n_3 + n_4)m \quad (15)$$

where n_o represents the base value for a straight, smooth and uniform channel in natural materials, n_1 represents an additive value that is accounting for surface irregularities, n_2 accounts for variation in channel geometry along the reach, n_3 accounts for the obstructions within the channel, n_4 represents an additive value for vegetative elements that have a net affect on the flow, and m the corrective factor for meandering channel.

Since vegetation on floodplains is larger than that found within the channel, its influence on flow resistance and flow depth plays a key role during overbank flooding. Thus, a method to evaluating flow resistance based on drag forces created by larger plants and woody vegetation was proposed by Petryk *et al.* (1975). Although this method bares some limitations (i.e. velocities within the channel must be minimal, vegetative elements must not bent or distorted) and assumes the forces involved are in longitudinal direction it is, still, a powerful roughness coefficient estimator because it takes into account all the crucial vegetation and channels parameters. That equation is,

$$n = n_o \sqrt{1.0 + \left(\frac{C_D \sum A_i}{2gAL} \right) \left(\frac{K}{n_o} \right)^2 \left(\frac{A}{P} \right)^{4/3}} \quad (16)$$

Here P is the wetted perimeter of the channel, A is the cross-sectional area of the flow in ft², $\sum A_i$ is the total frontal area of vegetation obstructing the flow, in ft², L represents the channel reach length in ft, the expression $\frac{C_D \sum A_i}{AL}$ represents the blockage of the vegetative elements or bulk density of vegetation in the floodplain.

Appendix E - Theoretical basis

In a thick, emergent, vegetative canopy, the resistance to flow through the stem elements is mostly dominated by drag forces imposed upon individual stems of the canopy. Thus, the formulae used in this portion of the thesis were derived from physical processes of flow through a vegetative canopy. The approach for acquiring roughness resistance information relative to vegetation using a theory-based approach is described below.

In principle, modeling water flow through a porous medium such as vegetative canopy involves a correction for the presence of vegetation within the body of water (Baptist, 2007). To correct this anomaly, the fraction of horizontal area occupied by the canopy stems A_p must be taken into account (Li *et al.*, 1973). Microscopic velocity (solidity) residing within the vegetative stems also helps not only to determine the flow resistance to roughness in the canopy, but also correct horizontal area when computing the flow shear stress or the bed shear stress, in that order.

$$A_p = 1/4 \pi D^2 m \quad (17)$$

where D is the vegetative stem diameter and m represents the number of cylinders per m^2 horizontal area or (m^{-2})

On the other hand, other experimental studies stipulated that the correction term mentioned previously can be neglected when calculating the vegetation roughness resistance in natural scenarios. The impact on neglecting the corrector is so insignificant that it has little to no affect on the experimental results James *et al.* (2004) to a point where it can be disregarded.

A dimensional analysis and modeling was offered by Fathi and Kouwen (1997), and it assumed that surface tension is not important parameter in dense emergent vegetation

when determining flow resistance. The dominant parameters for estimating resistance in the emergent and isolated plant flow in a canopy can be anticipated to be

$$f(C_d, A_o, V, \rho, y_m, J, \phi, \mu, g, h, l_1, \dots, l_n) = 0 \quad (18)$$

where C_d represents the drag coefficient, A_o is momentum absorbing area (MAA), V is mean channel stream velocity, ρ and μ are water density and viscosity, respectively, y_m is the normal flow depth (also called H in this thesis), g is the gravitational constant, $l_1 \dots l_n$ are the characteristic lengths defining spacing between stem elements or density of plants in vegetative canopy, flexural rigidity $J = EI$, where E is the modulus of elasticity of plant and I is the cross-sectional moment of inertia of the plant, Φ is a constant accounting for leaf incidence angle effects, and h is the average canopy heights.